Contribution from the Department of Geosciences, The Pennsylvania State University, University Park, Pennsylvania 16802, and Chemistry Division, Oak Ridge National Laboratory, Oak Ridge, Tennessee 37830

Hydrolysis Equilibria of Tungsten(VI) in Aqueous Sodium Chloride Solutions to 300 °C

D. WESOLOWSKI,*† S. E. DRUMMOND, R. E. MESMER,‡ and H. OHMOTO†

Received July 12, 1983

Formation constants for the protonated mononuclear and polynuclear forms of tungstate have been measured by means of a hydrogen electrode concentration cell from 95 to 290 °C in 0.10–5.1 *m* NaCl solutions over a pH range of 2–8 and tungsten concentration from 5×10^{-4} to 10^{-2} *m*. Polytungstates dominate the speciation in the 10^{-2} *m* solutions below a pH of 5, particularly in the low-temperature solutions. Monomers become increasingly stable at low tungsten concentrations, high temperatures, and high ionic strengths and are the only form of tungsten detected above 200 °C at 5.1 *m* NaCl. The equilibrium quotients for the reaction $WO_4^{2-} + H^+ \rightleftarrows HWO_4^-$ have been determined to 300 °C over the entire composition range. An analytical expression for the temperature and ionic strength dependence of these equilibrium quotients and derived thermodynamic properties are presented.

Introduction

Tungsten, a critically important strategic metal, is mined from deposits of scheelite, $CaWO_4$, and wolframite, $(Fe,Mn)WO_4$. In order to develop sound geochemical models for the genesis of these deposits, the speciation of tungsten in ore-forming solutions must be understood and quantified. Also the extraction of tungsten from ores involves dissolution of scheelite and wolframite at elevated temperatures and reprecipitation of various mononuclear and polynuclear products. Finally, tungstate acts as a catalyst in certain oxidation–reduction reactions. Knowledge of the species distribution at elevated temperatures may aid in increasing the efficiency of these processes.

Numerous studies of tungsten ores[1,2] indicate that the ore-forming solutions are typically aqueous NaCl brines with ionic strengths of 1–10 *m*, temperatures of 200–500 °C, and tungsten concentrations of around 10^{-5} *m*. It has been postulated[3,4] that WO_4^{2-}, HWO_4^-, and $H_2WO_4^0$ are the dominant forms of tungsten under these conditions. Due to the strong tendency for W(VI) to polymerize at low temperatures, the thermodynamic stabilities of the monomeric species are poorly known. Table I summarizes the previously measured equilibrium quotients relating the monomeric forms of W(VI).

At temperatures less than 100 °C, acidification of alkali tungstate solutions results in the formation of various polynuclear species. Sasaki[5,6] interpreted his potentiometric titrations of Na_2WO_4 solutions at 25 and 80 °C in 1 and 3 *m* $NaClO_4$ in terms of a series of hexamers, $H_nW_6O_{21}^{n-6}$, where $n = 1$–4. In a later refinement, Arnek and Sasaki[7] included $W_6O_{21}^{6-}$, H_2WO_4, and a dodecamer, $H_{14}(WO_4)_{12}^{10-}$, and achieved a statistically better fit to the same data. Aveston,[8] in a more detailed study of the hydrolysis of WO_4^{2-} in 3 M LiCl at 50 °C, used potentiometric titrations coupled with ultracentrifuge and Raman studies to determine that the species $H_7(WO_4)_6^{5-}$, $H_{14}(WO_4)_{12}^{10-}$, and $H_{18}(WO_4)_{12}^{6-}$ adequately explained his experimental results in acidic to mildly basic solutions at total tungsten concentrations of 0.2–0.005 M. The results of these and other studies are exhaustively reviewed by Kepert,[9] Baes and Mesmer,[10] and Tytko and Glemser.[11]

Throughout this paper, the symbol $Q_{x,y}$ will be used to represent the equilibrium quotient for the generalized reaction

$$yH^+ + xWO_4^{2-} \rightleftarrows H_y(WO_4)_x^{y-2x} \quad (1)$$

$$Q_{x,y} = [H_y(WO_4)_x^{y-2x}]/([H^+]^y[WO_4^{2-}]^x) \quad (2)$$

Table I. Equilibrium Quotients for Reactions Formulated according to Eq 1 and 2, Involving the Monomeric W(VI) Species

	lit. values					
this study log $Q_{1,1}$ [b]	log $Q_{1,1}$	log ($Q_{1,2}/Q_{1,1}$)	log $Q_{1,2}$	T, °C	ionic medium	ref
	~4.05	~4.05	8.1	20	0.1 M KCl	12
3.22 ± 0.53	~3.5	~4.6	8.1	20	0.1 M $NaClO_4$	13
3.62 ± 0.53	3.66	2.19	5.85	25	$I = 0.003$ *m*	14
3.62 ± 0.53	3.51	2.30	5.81	25	$I \approx 0$	15
2.63 ± 0.65	~3.8			22	3 M $NaNO_3$	16
			11.3	25	3 M $NaClO_4$	7
4.71 ± 0.06	4.73[a]			150[c]	$I \approx 0$	17

[a] Extrapolated to saturated vapor pressure according to the data of Krumhansl.[17] [b] From eq 11 and 12; uncertainty 3σ. [c] Vapor saturated.

where the units are molality.

As can be seen from Table I, there is fair agreement on the approximate value of $Q_{1,1}$ at room temperature, but $Q_{1,2}$ is very poorly established. Ivanova and Khodakovskiy[3,18] have extrapolated the 25 °C results of Yatsimirskii and Prik[15] to 350 °C at infinite dilution and vapor saturation using the correspondence principle for entropies of ions and comparing the first and second dissociation constants of tungstic acid, H_2WO_4, with those of other acids. They propose the following equations (T, K) for the first and second stepwise *association* constants of tungstic acid in pure water:

* Experimental work conducted while at Oak Ridge National Laboratory. To whom correspondence should be addressed at the Chemistry Division, Oak Ridge National Laboratory, Oak Ridge, TN 37830.
† The Pennsylvania State University.
‡ Oak Ridge National Laboratory.

(1) M. T. Einaudi, *Econ. Geol., 75th Anniv. Vol.*, 317 (1981).
(2) N. C. Higgins, *Can. J. Earth Sci.*, **17**, 823 (1980).
(3) G. F. Ivanova and I. L. Khodakovskiy, *Geokhimiya*, **8**, 426 (1968).
(4) V. F. Barabanov, *Int. Geol. Rev.*, **13** (3), 332 (1971).
(5) Y. Sasaki, *Acta Chem. Scand.*, **15** (7), 175 (1961).
(6) Y. Sasaki, *Proc. Int. Conf. Coord. Chem.* **7** (1962).
(7) R. Arnek and Y. Sasaki, *Acta Chem. Scand., Ser. A*, **A28** (1), 20 (1974).
(8) J. Aveston, *Inorg. Chem.*, **3**, 981 (1964).
(9) D. L. Kepert in "Comprehensive Inorganic Chemistry", Vol. 4, A. F. Trotman-Dickenson, et al., Eds., Pergamon Press, Oxford, 1973, Chapter 51.
(10) C. F. Baes, Jr., and R. E. Mesmer, "The Hydrolysis of Cations", Wiley, New York, 1976.
(11) K.-H. Tytko and O. Glemser, *Adv. Inorg. Chem.*, **19**, 239 (1976).
(12) G. von Schwarzenbach and J. Meier, *J. Inorg. Nucl. Chem.*, **8**, 302 (1958).
(13) G. von Schwarzenbach, G. Geier, and J. Littler, *Helv. Chim. Acta*, **45**, 2601 (1962).
(14) K. B. Yatsimirskii and V. F. Romanov, *Russ. J. Inorg. Chem.* (*Engl. Transl.*), **10** (7), 877 (1965).
(15) K. B. Yatsimirskii and K. E. Prik, *Russ. J. Inorg. Chem.* (*Engl. Transl.*), **9** (8), 995 (1964).
(16) K.-H. Tytko and O. Glemser, *Z. Naturforsch., B: Anorg. Chem., Org. Chem., Biochem., Biophys., Biol.*, **25B**, 429 (1970).
(17) J. L. Krumhansl, Ph.D. Thesis, Stanford University, 1976, p 111.
(18) G. F. Ivanova and I. L. Khodakovskiy, *Geokhimiya*, **11**, 1426 (1972).

0020-1669/84/1323-1120$01.50/0 © 1984 American Chemical Society

$$\log (K_{1,2}/K_{1,1}) = 1492.75/T - 9.766 + 0.0233T \quad (3)$$

$$\log K_{1,1} = 924.493/T - 5.3286 + 0.0199T \quad (4)$$

In this paper we present the results of potentiometric titrations of $Na-WO_4-Cl-H_2O$ solutions and establish the relationships among the monomeric and polynuclear forms of W(VI) in the range 100–300 °C, 0.1–5.1 *m* NaCl, and (5×10^{-4})–10^{-2} *m* total tungsten concentration at pressures slightly in excess of vapor saturation. These data were reduced to the most plausible set of species and stability constants by regression analysis. A mathematical model for the temperature and salinity dependence of $Q_{1,1}$ in NaCl media is presented.

Experimental Procedures

Materials. Stock solutions of about 5.2 *m* NaCl prepared from Fisher Scientific Co. Certified reagent grade NaCl were purified by acidifying with hydrochloric acid to pH 4.0 and sparging with argon to remove CO_2. After sparging, the solutions were again neutralized with a small amount of carbonate-free NaOH solution. NaOH reference solutions were prepared from Fisher Scientific Co. reagent grade 50% NaOH and NaCl stock solution. The tungstate solutions were prepared with use of biological grade $Na_2WO_4 \cdot 2H_2O$ from Alfa Products Co. and NaCl stock solution with enough 50% NaOH added to maintain a pH of 8–9 at ambient temperature. The HCl titrant solutions were prepared from Fisher Scientific Co. Certified reagent grade NaCl and Fisher Certified standard 0.1000 N HCl. The HCl solutions were sparged with argon to remove CO_2 after preparation.

The concentrations of the HCl titrant and NaOH reference solutions were verified by comparing the emf generated between the two solutions at experimental temperatures to the dissociation constant of water at the same conditions.

All solvents were stored under 99.998% argon. The NaCl stock and HCl titrant solutions were stored in glass vessels and the reference and tungstate solutions in heavy-walled polyethylene bottles. All solution containers were equipped with delivery tubes, and solutions were transferred by positive argon pressure to minimize contact with air. Tungstate solutions were transferred under argon to avoid CO_2 contamination.

After the solutions were sealed in the hydrothermal vessel, the system was purged of air by successively pressurizing with H_2 to 3.5 MPa and venting to the atmosphere. This operation was repeated 4–5 times before final pressurization with 0.7–1.4 MPa H_2. Ultrapure H_2 (99.999%) from Matheson Co. was used throughout these experiments.

Potentiometric Apparatus and Techniques. The stirred potentiometric concentration cell employed in this research is described in detail by Mesmer, Baes, and Sweeton.[19] Briefly, the apparatus consists of a pressure vessel housing a pair of Teflon cups containing matched hydrogen electrodes. The cups are connected through the fluid phase by a porous Teflon plug, and the vapor space is interconnected. Magnetic stirring bars in each compartment provide agitation. The original design was improved for long-term high-temperature experiments by isolating the electrode seals from the heat in extension tubes above the oil bath.

Titrant with compositions in the range 0.1–5.1 *m* NaCl, 0.1–0.01 *m* HCl was added to the test (outer cup) compartment through preheated platinum capillary tubing from a zircaloy positive-displacement pump.

Potentiometric Measurements. The potentiometric circuit previously described[19] consisted of a vibrating-reed electrometer and a precision potentiometer in series with the chemical cell. The cell representation before titrant is added is

$$\text{Pt, } H_2 \left| \begin{matrix} a \text{ m NaCl} \\ b \text{ m } WO_4^{2-} \\ c \text{ m NaOH} \end{matrix} \right| \left| \begin{matrix} a \text{ m NaCl} \\ \\ d \text{ m NaOH} \end{matrix} \right| H_2, \text{ Pt} \qquad \begin{matrix} \text{test} \\ \\ \\ \end{matrix} \quad \begin{matrix} \text{reference} \\ \\ \\ \end{matrix} \qquad (I)$$

The electrode compartment on the right (inner cup) contains the reference electrode. The hydrogen pressure is equal in both compartments. In these experiments *b* was varied from 0.0005 to 0.01 in the 1 *m* NaCl solutions to determine the species present. Then *a* was varied to 0.1 and 5.1 at $b = 0.001$ to determine the ionic strength dependence on the equilibria. The NaOH concentration in the reference, *d*, was fixed at 0.01, and NaOH was added to the test compartment to maintain a starting c/b ratio of 0.5–1.0. This ensured that the titrations were all started in the WO_4^{2-} dominant stability field.

The measured potential generally reached a stable value within 5–10 min after the addition of titrant at the beginning and end of the titration. However, in the middle of the titration at $\bar{n}$ of 0.3–1.0 ($\bar{n}$ is defined as the average number of protons chemically bound per WO_4^{2-} ion according to eq 6) the potential would typically drift for 10–15 min before stabilizing. This slow equilibration was more pronounced in the solutions with high tungsten concentration and low temperatures and probably corresponds to either the sluggish formation of polynuclear species from monomer or the rearrangement of the proportions of the polynuclear species. In the worst cases the drift would persist at a rate of 1–5 mV/h after as much as 30 min. The duration of the experiments was limited by the design of the cell to about 12 h. Therefore, some of the potentials recorded in the middle $\bar{n}$ range were drifting at a rate of a few millivolts per hour. This implies that equilibrium was not always fully established in the middle of the titration and results in an added uncertainty of as much as 10% in the equilibrium proton concentration in about 10% of the data. Consequently, uncertainties in the assignment of equilibrium speciation and formation constants are likely to be greatest in the middle $\bar{n}$ range. The magnitude of this additional uncertainty is probably not appreciably greater than the overall uncertainty associated with such titrations at optimum conditions.

This contention is supported by the excellent reproducibility of the experiments over the entire $\bar{n}$–pH range. Only the experiment at 150 °C, $I = 5.12$, and total tungsten concentration 10^{-3} *m* was unreproducible. This anomalous experiment was characterized by steady and continuing drifts of 10 mV/h and for several reasons discussed below was eliminated from the data set.

Titrations were conducted at 95, 150, 200, 250, and 290 °C and were continued until erratic potentials were encountered, signaling either that a precipitate formed or that the outer cup was filled. Precipitation commenced at lower $\bar{n}$ values at higher temperatures and total tungsten concentrations. The solids were not extensively investigated in this study but generally consisted of voluminous fluffy to pasty masses of deep blue material. Another solid form consisted of very small amounts of dense, purplish blue, acicular crystals. Four samples of the fluffy blue material were analyzed by X-ray powder diffraction. Three samples were essentially amorphous. The fourth (generated at 200 °C, $I = 1$ m, total tungstate concentration 0.01 *m*, and $\bar{n} \approx 1.7$) matched exactly the pattern reported by Freedman and Leber[20] for their tungsten phase C, $Na_2O \cdot (WO_3 \cdot {}^1/_2H_2O)_{8-40}$.

As mentioned above, the solids generated were always deep blue or purplish blue. Solutions containing these precipitates were usually clear and colorless. Solutions from runs terminated at $\bar{n}$ values less than ~0.5 were also typically clear and colorless. Solutions from runs terminated at higher $\bar{n}$ values, in which no precipitate occurred, were usually tinted blue to blue-gray, the intensity of the color varying from hardly visible to deep blue. The intensity of the color appeared to be directly related to tungsten concentration and inversely proportional to pH and temperature. No attempt was made to measure the visible spectra of these solutions, as the colors began to fade immediately upon exposure to air, often fading completely after a few minutes to hours.

These colors are apparently the result of partial reduction of W(VI) by molecular hydrogen to a mixed-valence-state polymer ("tungsten blues") having the same structure as the fully oxidized form but containing one or more W(V) atoms.[21,22] This reducibility is believed to be restricted to certain polyanion structures,[21] notably the dodecatungstates. The sodium tungstate salts generated in the experiments presumably contain a similar easily reducible dodecameric radical.

This reduction was a great concern to us in the early phases of the research, as it was feared that significant amounts of reduced tungsten were formed in the presence of the hydrogen. However, several lines of evidence indicate that the reduction was a stoichiometrically insignificant process:

(19) R. E. Mesmer, C. F. Baes, Jr., and F. H. Sweeton, *J. Phys. Chem.*, **74** (9), 1937 (1970).

(20) M. L. Freedman and S. Leber, *J. Less-Common Met.*, **7**, 427 (1964).
(21) M. T. Pope, *Inorg. Chem.*, **11** (8), 1973 (1972).
(22) J. M. Fruchart, et al., *J. Inorg. Nucl. Chem.*, **38**, 1627 (1976).

1. As described above, a solid phase was produced in one experimental run which, although deep blue, had an X-ray powder pattern identical with that of a fully oxidized sodium polytungstate reported in the literature.[20] When the conditions of this run were duplicated under an oxidized atmosphere, a white solid with an X-ray pattern identical with that of the blue compound was formed. This suggests that the blue solid was an oxidized form of tungsten colored by small amounts of reduced product.

2. Identical experimental runs were conducted under 0.7 and 3.5 MPa of H_2. The runs were terminated at various similar $\bar{n}$ values, and although the intensity of the blue color was much greater in the 3.5-MPa H_2 runs, the titration curves were essentially identical with those of the 0.7-MPa runs, within the accuracy of the data.

3. As a common practice, about 0.5 MPa of H_2 was quickly introduced into the vessel to alleviate a blocked liquid junction. However, after time was allowed for the added H_2 to equilibrate with the solutions (15–30 min), the potential returned to the previous value within a few tenths of a millivolt.

These observations suggest that for our experimental conditions (0.7–3.5 MPa of H_2) the reduction process did not involve a significant change in either the hydrogen ion concentration in the cell or the major tungsten speciation and that any major reduction could only have occurred during quenching of the runs. The data analysis presented below will demonstrate that the results obtained in this study are readily relatable to those of other studies conducted in oxidizing systems. Thus, our results are applicable to oxidizing systems as well as the relatively reducing conditions often encountered in certain geological and industrial environments.

Data Reduction

Stoichiometric molalities of all species in both compartments were computed at each point in the titrations. Corrections were applied for the small amount of water vaporized from the solutions to the gas phase. This correction amounted to less than 1% at the highest temperature.

The potential E for the cell (I) is given by the expression

$$E = (RT/F) \ln ([OH^-]/[OH^-]_r) - \sum D_i([i]_r - [i]) \qquad (5)$$

where $[OH^-]$ denotes the molal concentration of hydroxide ion, [i] denotes the concentration of each ionic species in the solutions, including hydroxide, and the subscript r refers to the reference solution. The term $\sum D_i([i]_r - [i])$ represents the liquid-junction potential, calculated from the Henderson equation.[10,19] The limiting equivalent conductances of the ionic species involved, which determine the D_i values, were taken from the data of Quist and Marshall,[23] with the approximations that the equivalent conductance of WO_4^{2-} equals that of SO_4^{2-} and that of HWO_4^- (and all other hydrolysis products) equals that of HSO_4^-. Since the molal ratio of supporting electrolyte to total tungsten was always ≥ 100, the liquid-junction term in eq 5 was generally less than 1 mV at the higher salinities and less than 3 mV in the 0.1 m NaCl runs.

The data analysis and interpretation techniques used in this study have been extensively discussed in previous papers.[24–27] The average number of protons bound per tungstate anion at each observation point, $\bar{n}_o$, is calculated by using the equation

$$\bar{n}_o = (m(H^+) - [H^+] + [OH^-])/m(WO_4^{2-}) \qquad (6)$$

where $m(H^+)$ and $m(WO_4^{2-})$ are the formal stoichiometric concentrations of acid and tungstate, $[OH^-]$ is obtained from an iterative solution of eq 5, and $[H^+]$ is calculated from the $[OH^-]$ values by using the data on the dissociation constant of water, Q_w, in NaCl media reported by Busey and Mesmer.[28]

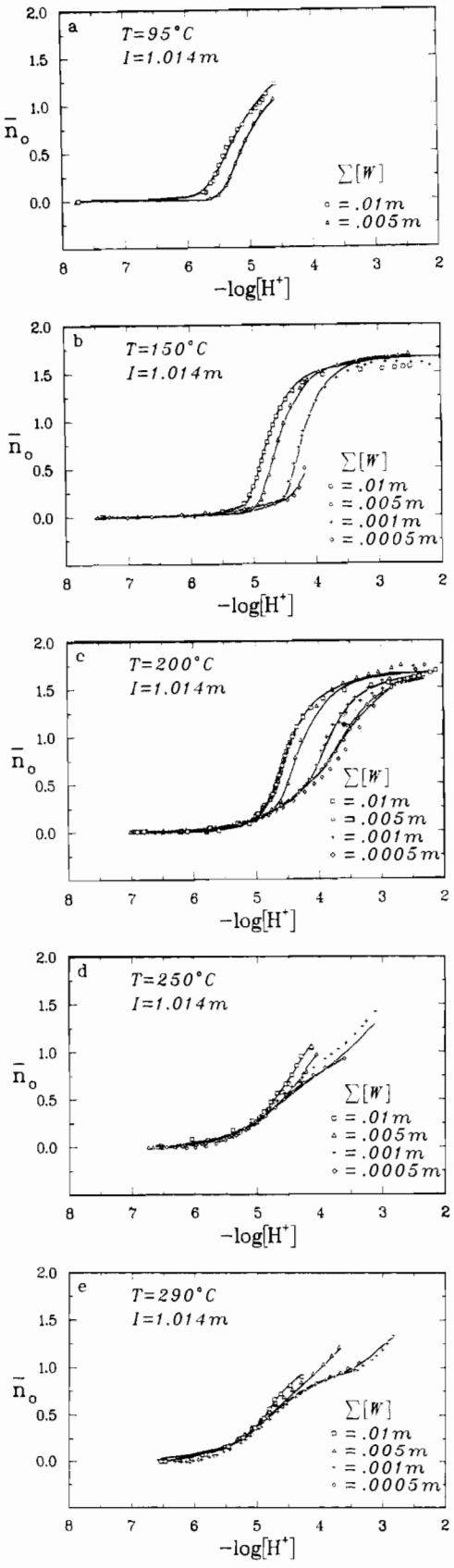

Figure 1. $\bar{n}$ vs. −log $[H^+]$ (defined as pH in Data Reduction) curves for W(VI) hydrolysis in 1.014 m NaCl solutions from 95 to 290 °C. Experimental data ($\bar{n}_o$) are plotted for tungsten concentrations of 0.01, 0.005, 0.001, and 0.0005 m. Solid lines are smoothed curves through the calculated $\bar{n}_c$ values for each data point (eq 7, scheme A, Table IV).

(23) A. S. Quist and W. L. Marshall, *J. Phys. Chem.*, **69**, 2984 (1964).
(24) R. E. Mesmer and C. F. Baes, Jr., *Inorg. Chem.*, **6** (11), 1951 (1967).
(25) R. H. Busey and R. E. Mesmer, *Inorg. Chem.*, **16**, 2444 (1977).
(26) R. E. Mesmer and C. F. Baes, Jr., *J. Solution Chem.*, **3**, 307 (1974).
(27) R. E. Mesmer, C. F. Baes, Jr., and F. H. Sweeton, *Inorg. Chem.*, **11**, 537 (1972).
(28) R. H. Busey and R. E. Mesmer, *J. Chem. Eng. Data*, **23** (2), 175 (1978).

Table II. Hydrolysis Results for WO_4^{2-} in NaCl Solutions, $I = 1.014$ *m*

$\bar{n}_o$	$-\log h^+$	$m_{WO_4^{2-}} \times 10^3$	$\bar{n}_o$	$-\log h^+$	$m_{WO_4^{2-}} \times 10^3$	$\bar{n}_o$	$-\log h^+$	$m_{WO_4^{2-}} \times 10^3$	$\bar{n}_o$	$-\log h^+$	$m_{WO_4^{2-}} \times 10^3$	$\bar{n}_o$	$-\log h^+$	$m_{WO_4^{2-}} \times 10$
----------200 °C----------									--------150 °C---------			--------290 °C---------		
0.000±.007	7.016	5.027	0.000±.026	6.827	.4978	0.000±.024	6.722	1.021	0.000±.011	7.307	.4976	0.000±.007	6.538	10.10
0.002±.007	6.922	5.021	-0.009±.026	6.792	.4977	0.003±.024	6.673	1.021	-0.007±.011	7.015	.4940	0.001±.007	6.533	10.10
0.006±.007	6.747	5.012	-0.009±.026	6.714	.4975	0.000±.024	6.405	1.020	-0.001±.011	6.631	.4916	0.074±.007	5.815	9.996
0.012±.007	6.488	5.002	-0.005±.026	6.627	.4972	0.103±.024	5.145	1.018	0.021±.011	6.152	.4900	0.170±.007	5.460	9.893
0.022±.007	6.124	4.993	0.000±.026	6.472	.4969	0.253±.024	4.623	1.017	0.039±.011	5.774	.4892	0.267±.007	5.225	9.793
0.036±.007	5.781	4.984	0.013±.026	6.192	.4965	0.398±.024	4.330	1.015	0.060±.011	5.305	.4884	0.365±.008	5.036	9.694
0.045±.007	5.654	4.979	0.041±.026	5.686	.4960	0.544±.024	4.163	1.013	0.071±.011	5.149	.4880	0.464±.008	4.897	9.597
0.071±.007	5.385	4.965	0.088±.026	5.283	.4957	0.690±.024	4.042	1.011	0.082±.011	5.020	.4876	0.562±.008	4.809	9.501
0.089±.007	5.264	4.956	0.129±.026	5.076	.4954	0.841±.025	3.966	1.010	0.103±.011	4.813	.4868	0.661±.009	4.728	9.408
0.124±.007	5.077	4.938	0.170±.026	4.921	.4952	0.985±.025	3.878	1.008	0.123±.011	4.669	.4860			
0.160±.007	4.938	4.920	0.224±.026	4.740	.4949	1.117±.025	3.775	1.006	0.163±.011	4.465	.4844	0.000±.007	6.462	10.07
0.232±.007	4.758	4.884	0.278±.026	4.607	.4945	1.232±.026	3.656	1.005	0.209±.011	4.356	.4829	0.073±.007	5.870	9.969
0.322±.007	4.613	4.841	0.326±.026	4.468	.4942	1.325±.026	3.529	1.003	0.289±.011	4.274	.4805	0.162±.007	5.513	9.872
0.504±.008	4.497	4.755	0.417±.026	4.324	.4936	1.402±.027	3.412	1.001	0.498±.012	4.190	.4752	0.254±.007	5.276	9.778
0.777±.009	4.376	4.633	0.487±.026	4.200	.4931	1.495±.030	3.202	.9978				0.347±.007	5.088	9.685
1.315±.011	4.029	4.406	0.542±.027	4.112	.4927	1.577±.038	2.981	.9928	0.000±.024	7.182	1.020	0.439±.008	4.933	9.593
1.482±.012	3.782	4.335	0.645±.027	3.958	.4919	1.645±.054	2.746	.9845	0.356±.024	4.449	1.015	0.532±.008	4.813	9.504
1.553±.013	3.599	4.300	0.692±.027	3.891	.4914	1.726±.093	2.479	.9684	0.836±.024	4.227	1.010	0.625±.008	4.724	9.416
1.607±.013	3.385	4.266	0.738±.028	3.833	.4910							0.718±.009	4.632	9.329
1.644±.014	3.193	4.233	0.830±.028	3.733	.4902	0.000±.012	6.772	1.021	0.000±.026	7.260	1.021	0.810±.009	4.475	9.245
1.671±.015	3.042	4.200	0.951±.030	3.603	.4890	-0.005±.012	6.716	1.020	-0.009±.026	7.197	1.020	0.901±.009	4.294	9.161
1.712±.018	2.829	4.135	1.064±.032	3.498	.4878	-0.001±.012	6.563	1.020	0.048±.026	5.282	1.019			
1.744±.021	2.683	4.073	1.177±.035	3.370	.4861	0.005±.012	6.348	1.019	0.202±.026	4.518	1.017	0.000±.013	6.311	1.014
			1.323±.042	3.222	.4837	0.016±.012	6.010	1.018	0.374±.026	4.428	1.015	-0.006±.013	6.210	1.013
0.000±.007	6.904	10.06	1.402±.051	3.095	.4813	0.040±.012	5.572	1.017	0.546±.026	4.360	1.013	-0.006±.013	6.132	1.012
0.002±.007	6.798	10.05	1.449±.066	2.959	.4782	0.074±.012	5.266	1.016	0.716±.026	4.277	1.011	0.007±.013	6.021	1.011
0.081±.007	5.115	9.957	1.498±.085	2.833	.4743	0.110±.012	5.055	1.015	0.887±.026	4.211	1.009	0.021±.013	5.885	1.011
0.183±.007	4.976	9.857	1.545±.105	2.737	.4705	0.147±.012	4.904	1.014	1.049±.026	4.105	1.008	0.043±.013	5.758	1.010
0.385±.008	4.741	9.662	1.585±.125	2.658	.4667	0.183±.012	4.783	1.014	1.206±.027	3.997	1.006	0.071±.013	5.641	1.009
0.486±.008	4.685	9.568	1.592±.168	2.532	.4594	0.220±.013	4.681	1.013	1.344±.027	3.849	1.004	0.102±.013	5.532	1.008
0.588±.008	4.637	9.475	1.688±.210	2.442	.4523	0.257±.013	4.596	1.012	1.447±.027	3.663	1.002	0.136±.013	5.434	1.007
0.689±.009	4.589	9.385	1.735±.296	2.304	.4387	0.328±.013	4.443	1.010	1.514±.028	3.482	1.000	0.207±.013	5.258	1.005
0.791±.009	4.539	9.296				0.399±.013	4.321	1.008	1.553±.030	3.330	.9986	0.244±.013	5.183	1.004
0.892±.009	4.483	9.208	0.000±.012	6.859	.4977	0.470±.013	4.234	1.007	1.575±.032	3.205	.9968	0.281±.013	5.111	1.004
0.993±.010	4.421	9.122	-0.006±.012	6.844	.4976	0.543±.013	4.165	1.005	1.596±.034	3.108	.9950	0.356±.013	4.976	1.002
1.094±.010	4.346	9.038	-0.007±.012	6.821	.4972	0.687±.013	4.053	1.002	1.608±.044	2.887	.9898			
1.194±.011	4.251	8.956	-0.008±.012	6.772	.4963	0.897±.014	3.902	.9967	1.609±.060	2.701	.9828	0.000±.013	6.288	1.017
1.294±.011	4.123	8.874	-0.008±.012	6.720	.4955	1.138±.015	3.673	.9901	1.598±.095	2.473	.9692	-0.003±.013	6.185	1.016
1.390±.012	3.925	8.795	-0.008±.012	6.592	.4939	1.238±.016	3.560	.9869	1.600±.140	2.300	.9527	0.071±.013	5.660	1.013
1.475±.012	3.583	8.717	-0.007±.012	6.514	.4930	1.365±.019	3.326	.9805	1.569±.188	2.178	.9368	0.215±.013	5.245	1.009
1.526±.013	3.154	8.640	-0.002±.012	6.371	.4918	1.438±.024	3.143	.9741	1.657±.280	2.018	.9064	0.294±.014	5.088	1.007
1.554±.014	2.878	8.564	0.002±.012	6.248	.4910	1.488±.032	2.974	.9663				0.375±.014	4.944	1.005
1.575±.015	2.699	8.490	0.007±.012	6.087	.4902	1.530±.045	2.806	.9555	0.000±.007	7.496	5.022	0.455±.014	4.806	1.003
1.591±.016	2.569	8.417	0.011±.012	5.992	.4898	1.550±.055	2.716	.9480	0.006±.007	6.857	5.000	0.535±.014	4.672	1.001
1.606±.018	2.468	8.345	0.019±.012	5.837	.4892	1.570±.065	2.643	.9406	0.015±.007	6.120	4.991	0.612±.014	4.533	.9995
1.619±.020	2.386	8.275	0.032±.012	5.646	.4886	1.582±.075	2.580	.9333	0.032±.007	5.705	4.982	0.686±.014	4.390	.9976
1.632±.022	2.319	8.205	0.042±.012	5.526	.4882	1.602±.096	2.478	.9190	0.049±.007	5.195	4.973	0.755±.014	4.239	.9958
1.658±.026	2.211	8.070	0.065±.012	5.313	.4874				0.067±.007	5.083	4.964	0.816±.014	4.081	.9940
1.680±.031	2.125	7.939	0.090±.012	5.144	.4866	0.000±.007	6.825	10.05	0.085±.007	5.010	4.955	0.865±.015	3.922	.9922
			0.116±.012	5.009	.4858	0.004±.007	6.793	10.05	0.121±.007	4.940	4.937	0.904±.015	3.777	.9904
0.000±.007	6.929	10.04	0.169±.012	4.803	.4842	0.041±.007	5.742	9.993	0.176±.007	4.882	4.910	0.933±.016	3.651	.9886
0.001±.007	6.866	10.04	0.208±.012	4.683	.4830	0.087±.007	5.303	9.946	0.249±.007	4.836	4.875	0.979±.017	3.458	.9850
0.070±.007	5.272	9.950	0.246±.012	4.581	.4818	0.180±.007	4.991	9.854	0.432±.008	4.753	4.788	1.019±.019	3.321	.9815
0.156±.007	5.018	9.864	0.320±.012	4.411	.4795	0.273±.007	4.874	9.763	0.615±.008	4.681	4.705	1.081±.023	3.175	.9762
0.243±.007	4.901	9.780	0.410±.013	4.228	.4764	0.367±.007	4.768	9.674	0.798±.009	4.603	4.625	1.127±.026	3.102	.9727
0.330±.007	4.781	9.697	0.491±.013	4.077	.4733	0.460±.008	4.702	9.587	0.980±.010	4.517	4.548	1.189±.030	3.010	.9675
0.416±.007	4.713	9.616	0.562±.014	3.948	.4703	0.554±.008	4.654	9.501	1.161±.011	4.406	4.473	1.254±.035	2.935	.9624
0.520±.008	4.658	9.520	0.645±.015	3.820	.4666	0.647±.008	4.608	9.417	1.341±.012	4.248	4.400	1.338±.043	2.829	.9540
0.607±.008	4.615	9.441	0.755±.017	3.684	.4615	0.741±.009	4.564	9.334	1.428±.012	4.127	4.365			
			0.850±.020	3.570	.4565	0.834±.009	4.518	9.252	1.511±.012	3.949	4.330	0.000±.012	6.289	.4984
0.000±.007	6.958	10.05	1.083±.030	3.343	.4429	0.928±.009	4.464	9.172	1.577±.013	3.652	4.296	-0.001±.012	6.070	.4946
0.537±.008	4.665	9.510	1.308±.049	3.116	.4238	1.021±.010	4.406	9.094	1.609±.013	3.320	4.262	0.016±.012	5.931	.4926
			1.591±.093	2.860	.3903	1.207±.011	4.255	8.941	1.625±.014	3.101	4.229	0.061±.012	5.685	.4897
									1.650±.017	2.841	4.164	0.135±.012	5.442	.4867
--------95 °C---------			----------250 °C----------						1.670±.021	2.680	4.101	0.226±.012	5.232	.4839
									1.698±.026	2.517	4.010	0.357±.013	4.984	.4801
												0.457±.013	4.815	.4772
0.000±.007	7.749	10.06	0.000±.010	6.430	.4973	0.000±.024	6.359	1.020	0.000±.007	7.435	10.04	0.586±.013	4.598	.4735
0.087±.007	5.750	9.971	-0.001±.010	6.315	.4956	0.016±.024	6.019	1.019	-0.001±.007	7.398	10.04	0.729±.013	4.331	.4690
0.180±.007	5.635	9.880	-0.011±.010	6.135	.4939				0.007±.007	5.964	10.01	0.836±.014	4.066	.4646
0.273±.007	5.559	9.790	-0.004±.010	5.989	.4926	0.000±.007	6.671	5.036	0.131±.007	5.157	9.886	0.903±.016	3.845	.4602
0.367±.007	5.495	9.702	0.011±.010	5.822	.4914	0.017±.007	6.184	5.009	0.221±.007	5.070	9.799	0.947±.018	3.679	.4559
0.460±.008	5.434	9.615	0.035±.010	5.662	.4901	0.080±.007	5.582	4.970	0.310±.007	5.007	9.714	0.991±.021	3.561	.4517
0.553±.008	5.367	9.530	0.071±.010	5.513	.4889	0.117±.007	5.405	4.951	0.400±.007	4.953	9.630	1.048±.028	3.380	.4435
0.646±.008	5.286	9.447	0.123±.010	5.336	.4872				0.489±.008	4.912	9.548			
0.739±.009	5.195	9.365	0.180±.010	5.183	.4856	0.000±.007	6.745	5.037	0.579±.008	4.872	9.467	0.000±.008	6.542	5.048
0.925±.009	4.969	9.205	0.238±.010	5.049	.4839	0.040±.007	5.883	4.989	0.668±.008	4.831	9.388	0.016±.008	6.287	5.024
1.018±.010	4.832	9.127	0.326±.011	4.872	.4815	0.075±.007	5.632	4.969	0.776±.009	4.783	9.294	0.042±.008	6.052	5.002
			0.412±.011	4.715	.4791	0.111±.007	5.447	4.950	0.865±.009	4.738	9.217	0.074±.008	5.852	4.981
0.000±.006	8.106	10.06	0.497±.011	4.573	.4767	0.149±.007	5.307	4.930	0.955±.010	4.688	9.142	0.111±.008	5.694	4.959
0.083±.006	5.712	9.963	0.576±.011	4.435	.4744	0.205±.007	5.141	4.902	1.044±.010	4.631	9.068	0.149±.008	5.562	4.938
0.201±.007	5.592	9.848	0.672±.011	4.263	.4713	0.262±.008	5.006	4.873	1.133±.010	4.566	8.995	0.188±.008	5.452	4.917
0.286±.007	5.524	9.766	0.753±.012	4.102	.4682	0.319±.008	4.891	4.845	1.222±.011	4.481	8.923	0.248±.008	5.322	4.886
0.456±.007	5.408	9.608	0.831±.013	3.918	.4644	0.414±.008	4.723	4.799	1.311±.011	4.372	8.852	0.308±.008	5.201	4.855
0.625±.008	5.275	9.455	0.885±.015	3.762	.4607	0.490±.008	4.607	4.763	1.398±.012	4.205	8.783	0.368±.008	5.094	4.825
0.794±.009	5.111	9.306	0.928±.018	3.612	.4563	0.603±.009	4.452	4.710	1.480±.012	3.886	8.714	0.449±.008	4.958	4.785
0.963±.009	4.892	9.162				0.697±.009	4.321	4.666	1.525±.012	3.284	8.647	0.529±.008	4.831	4.746
1.048±.010	4.790	9.092	0.000±.023	6.347	1.019	0.790±.009	4.219	4.623	1.540±.013	2.937	8.580	0.609±.009	4.706	4.707
1.216±.011	4.605	8.955	0.001±.023	6.175	1.019	0.977±.010	4.056	4.540	1.548±.014	2.736	8.515	0.689±.009	4.579	4.669
			0.050±.023	5.786	1.018				1.556±.016	2.599	8.451	0.769±.009	4.449	4.632
0.000±.007	8.351	5.018	0.108±.023	5.521	1.017	0.000±.007	6.513	10.06	1.561±.017	2.494	8.387	0.847±.010	4.306	4.595
0.002±.007	7.783	4.999	0.181±.023	5.282	1.016	-0.005±.007	6.358	10.06				0.943±.010	4.116	4.550
0.023±.007	5.646	4.982	0.256±.023	5.106	1.015	0.074±.007	5.792	9.966				1.037±.011	3.950	4.505
0.057±.007	5.509	4.965	0.332±.024	4.952	1.015	0.165±.007	5.273	9.872	--------250 °C---------			1.129±.011	3.815	4.462
0.162±.007	5.387	4.914	0.416±.024	4.799	1.014	0.295±.007	4.976	9.744				1.221±.011	3.703	4.419
0.248±.007	5.323	4.872	0.484±.024	4.684	1.013	0.388±.007	4.831	9.654	0.000±.007	6.594	10.07			
0.387±.008	5.233	4.807	0.559±.024	4.564	1.012	0.481±.008	4.740	9.566	0.013±.007	6.546	10.05			
0.509±.008	5.154	4.751	0.632±.024	4.450	1.011	0.573±.008	4.614	9.479	0.086±.007	6.045	9.965	--------250 °C---------		
0.630±.008	5.070	4.697	0.730±.024	4.282	1.010	0.666±.008	4.503	9.395	0.178±.007	5.387	9.867			
0.803±.009	4.929	4.621	0.833±.024	4.099	1.009				0.274±.007	5.089	9.771	0.000±.026	6.456	.4975
0.924±.010	4.814	4.570	0.924±.024	3.921	1.007				0.371±.007	4.897	9.678	0.006±.026	6.199	.4967
1.061±.010	4.624	4.512	0.974±.024	3.818	1.006				0.468±.008	4.788	9.585	0.021±.026	5.980	.4963
			1.028±.025	3.707	1.005				0.564±.008	4.689	9.495	0.039±.026	5.823	.4960
			1.093±.025	3.581	1.004				0.661±.008	4.552	9.406	0.065±.026	5.660	.4958
			1.185±.026	3.436	1.002				0.757±.009	4.452	9.319	0.125±.026	5.410	.4954
			1.267±.027	3.318	1.000				0.854±.009	4.375	9.234	0.195±.026	5.207	.4949
			1.318±.029	3.252	.9987				0.950±.010	4.302	9.150	0.268±.026	5.033	.4945
			1.424±.032	3.109	.9954				1.045±.010	4.133	9.068			

It should be noted here that $[H^+]$ and $[OH^-]$ are also stoichiometric quantities. Effects of HCl and NaOH ion-pairing and ionic strength effects on activity coefficients are incorporated in the Q/K ratios for water dissociation.[28] Thus, pH is defined throughout this paper as the negative logarithm of the stoichiometric proton concentration, rather than activity.

Table III. WO_4^{2-} Hydrolysis Results at $I = 0.104$ and 5.120 m in NaCl Media

$\bar{n}_o$	$-\log H^+$	$mWO_4^{2-} \times 10^3$
I=0.104m		
150 °C		
0.000±.033	8.361	1.013
-0.008±.033	8.228	.9877
-0.025±.032	7.928	.9525
-0.028±.032	7.661	.9358
-0.027±.032	6.950	.9197
-0.018±.032	6.549	.9165
0.019±.032	5.570	.9118
0.053±.032	5.292	.9087
0.086±.032	5.066	.9056
0.120±.032	4.931	.9026
0.169±.032	4.770	.8980
0.221±.033	4.673	.8935
0.274±.033	4.626	.8890
0.407±.033	4.536	.8781
0.630±.033	4.435	.8604
0.807±.033	4.352	.8467
1.140±.033	4.120	.8207
1.270±.034	3.921	.8082
1.360±.034	3.710	.7962
1.390±.035	3.613	.7903
1.413±.035	3.527	.7845
1.443±.037	3.384	.7731
200 °C		
0.000±.032	7.951	1.014
-0.007±.032	7.794	.9848
-0.008±.032	7.663	.9668
-0.012±.032	7.479	.9495
-0.012±.032	7.178	.9329
-0.006±.032	6.915	.9247
0.012±.032	6.390	.9167
0.047±.032	5.953	.9120
0.079±.032	5.735	.9089
0.121±.032	5.534	.9050
0.165±.032	5.379	.9012
0.209±.032	5.251	.8974
0.254±.032	5.141	.8936
0.342±.032	4.956	.8861
0.429±.032	4.799	.8788
0.514±.032	4.652	.8716
0.597±.032	4.512	.8645
0.757±.033	4.279	.8506
0.914±.033	4.119	.8372
0.990±.033	4.045	.8307
1.127±.033	3.890	.8179
1.240±.034	3.730	.8055
1.346±.034	3.608	.7934
250 °C		
0.000±.033	7.755	1.018
-0.011±.033	7.579	.9841
-0.018±.033	7.427	.9644
-0.019±.033	7.212	.9455
-0.019±.033	7.050	.9364
-0.010±.033	6.825	.9274
-0.001±.033	6.672	.9229
0.017±.033	6.496	.9186
0.081±.033	6.142	.9099
0.123±.033	5.995	.9056
0.168±.033	5.868	.9014
0.261±.033	5.652	.8931
0.358±.033	5.471	.8849
0.455±.033	5.308	.8768
0.552±.033	5.145	.8690
0.647±.033	4.978	.8612
0.741±.033	4.791	.8536
0.828±.033	4.574	.8461
0.903±.033	4.320	.8388
0.959±.034	4.073	.8315
1.010±.034	3.904	.8244
1.081±.034	3.742	.8147
1.158±.035	3.609	.8038
1.227±.036	3.460	.7907
1.331±.038	3.308	.7717
1.444±.041	3.206	.7536
1.435±.044	3.114	.7421
I=0.104m		
290 °C		
0.000±.034	7.728	1.028
0.020±.034	7.583	.9940
0.002±.034	7.312	.9587
0.005±.034	7.084	.9409
0.034±.034	6.787	.9258
0.087±.034	6.527	.9154
0.127±.034	6.408	.9102
0.171±.034	6.287	.9051
0.269±.034	6.069	.8951
0.375±.034	5.870	.8854
0.441±.034	5.759	.8796
0.529±.034	5.609	.8720
0.618±.034	5.452	.8646
0.707±.034	5.277	.8572
0.795±.034	5.066	.8500
0.878±.035	4.791	.8429
0.914±.035	4.617	.8395
0.951±.035	4.382	.8351
0.976±.035	4.164	.8308
0.996±.035	3.998	.8266
1.013±.035	3.875	.8224
1.052±.035	3.710	.8141
1.094±.036	3.596	.8060
1.140±.036	3.512	.7981
1.216±.038	3.372	.7827
1.319±.041	3.222	.7606
1.512±.045	3.109	.7330
I=5.120m		
150 °C		
0.000±.022	8.111	1.008
-0.001±.022	7.949	1.004
0.017±.022	7.661	1.000
0.031±.022	7.409	.9982
0.050±.022	6.833	.9962
0.076±.022	5.894	.9951
0.115±.022	5.143	.9942
0.159±.022	4.886	.9932
0.306±.022	4.801	.9902
0.500±.022	4.668	.9863
0.694±.022	4.560	.9824
0.885±.022	4.441	.9786
1.071±.023	4.310	.9748
1.342±.023	4.115	.9691
1.552±.024	3.786	.9634
1.709±.025	3.523	.9579
1.786±.028	3.292	.9524
1.850±.032	3.136	.9470
1.920±.038	2.985	.9398
0.000±.030	8.271	.9925
-0.004±.030	8.144	.9887
0.002±.030	8.052	.9863
0.009±.030	7.938	.9840
0.018±.029	7.787	.9817
0.031±.029	7.565	.9795
0.054±.029	7.167	.9772
0.113±.029	5.986	.9749
0.162±.030	5.115	.9738
0.216±.030	4.909	.9727
0.333±.030	4.834	.9704
0.451±.030	4.824	.9682
0.685±.030	4.731	.9638
1.029±.030	4.505	.9572
1.356±.031	4.226	.9507
1.547±.031	3.984	.9464
1.684±.032	3.703	.9422
1.761±.033	3.458	.9380
1.811±.035	3.282	.9338
1.852±.037	3.153	.9297
1.927±.044	2.972	.9215
I=5.120m		
200 °C		
0.000±.022	7.322	1.010
0.011±.022	7.062	1.005
0.025±.022	6.906	1.003
0.038±.022	6.659	1.001
0.058±.022	6.135	.9985
0.122±.022	5.121	.9965
0.210±.022	4.694	.9944
0.298±.022	4.466	.9924
0.385±.022	4.305	.9903
0.479±.022	4.234	.9883
0.671±.022	4.146	.9842
0.850±.023	4.010	.9802
1.093±.023	3.794	.9743
1.307±.024	3.599	.9684
1.451±.025	3.444	.9635
1.555±.028	3.297	.9587
1.645±.031	3.149	.9530
1.710±.035	3.028	.9474
0.000±.022	7.303	1.010
0.014±.022	7.079	1.006
0.070±.021	6.301	.9993
0.128±.021	5.489	.9972
0.217±.022	4.891	.9951
0.305±.022	4.548	.9930
0.485±.022	4.247	.9889
0.678±.022	4.143	.9848
0.944±.022	3.926	.9786
1.178±.023	3.710	.9726
1.344±.024	3.627	.9686
250 °C		
0.000±.021	6.573	1.015
0.020±.021	6.419	1.011
0.032±.021	6.272	1.009
0.046±.021	6.059	1.007
0.073±.021	5.718	1.005
0.140±.021	5.351	1.002
0.223±.021	4.956	1.000
0.320±.021	4.757	.9980
0.414±.021	4.545	.9958
0.506±.021	4.376	.9936
0.638±.021	4.160	.9904
0.763±.022	3.980	.9871
0.913±.022	3.776	.9828
1.037±.023	3.592	.9786
1.139±.024	3.438	.9744
1.333±.026	3.313	.9681
1.475±.029	3.183	.9620
1.607±.034	3.029	.9538
1.700±.044	2.871	.9439
1.787±.057	2.733	.9322
1.889±.080	2.569	.9134
290 °C		
0.000±.029	6.167	1.038
0.222±.029	5.214	1.019
0.314±.029	4.938	1.016
0.417±.029	4.637	1.013
0.528±.029	4.404	1.010
0.637±.029	4.214	1.007
0.742±.029	4.047	1.004
0.840±.029	3.900	1.001
0.928±.030	3.765	.9986
1.004±.030	3.639	.9957
1.070±.031	3.527	.9929
1.127±.031	3.427	.9900
1.172±.032	3.334	.9872
1.214±.033	3.257	.9844
1.267±.036	3.117	.9789

The observed $\bar{n}$ and pH data are plotted in Figures 1 and 2 and listed in Tables II and III. Although the shapes of the initial $\bar{n}_o$–pH plots (Figures 1 and 2) indicate that the titrations all commenced well into the WO_4^{2-} dominant stability field (long tails at fairly constant $\bar{n}_o$ values near zero), many of the starting $\bar{n}_o$ values fell in the range 0.0 to −0.05 and in some runs ranged from +0.05 to −0.10. This deviation from zero was attributed to (a) inaccuracy in determining $m(H^+)$ in the test solutions and (b) protolytic impurities such as CO_2 in the test solutions. To normalize the curves, the initial $m(H^+)$ values were recalculated to give $\bar{n}_o = 0.0$ for the solution prior to titrant addition.

Table IV. Scheme A for WO_4^{2-} Hydrolysis in NaCl Solutions (Errors Represent 3σ)

I, m	T, °C	log $Q_{x,y}$[a] (1,1)	(1,2)	(6,7)	(6,10)	(12,18)	agreement factor $\sigma(\bar{n})$
5.120	200.0	4.06 ± 0.12	7.64 ± 0.12			107.93 ± 1.50	1.997
	250.0	4.31 ± 0.09	7.42 ± 0.12				1.855
	290.0	4.46 ± 0.08	7.27 ± 0.11				1.094
1.014	95.0			48.14 ± 0.06		117.33 ± 0.36	2.647
	150.0	3.80 ± 0.12		44.33 ± 0.18	58.05 ± 0.18	111.23 ± 0.18	2.595
	200.0	4.17 ± 0.03		42.78 ± 0.18	55.90 ± 0.18	107.20 ± 0.15	2.424
	250.0	4.58 ± 0.03		43.09 ± 0.21	55.55 ± 0.24		2.619
	290.0	4.78 ± 0.03		44.09 ± 0.24	55.81 ± 0.30		2.837
0.104	150.0	4.09 ± 0.06				115.53 ± 0.18	0.435
	200.0	4.68 ± 0.03			59.31 ± 0.09		0.268
	250.0	5.21 ± 0.03			60.74 ± 0.33		0.604
	290.0	5.64 ± 0.03			62.69 ± 0.24		0.440

[a] Figures in parentheses are the x and y values, respectively, for each species.

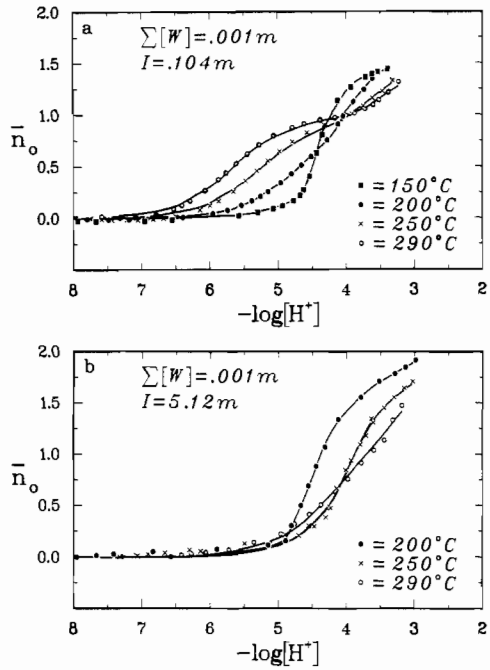

Figure 2. $\bar{n}$ vs. −log [H^+] (defined as pH in Data Reduction) curves for W(VI) hydrolysis in 0.104 m NaCl solutions at 150, 200, 250, and 290 °C (a) and in 5.12 m NaCl solutions at 200, 250, and 290 °C (b). All of the data are for 0.001 m tungsten. Solid lines are smoothed curves through the calculated $\bar{n}_c$ values (eq 7, scheme A, Table IV).

The $\bar{n}$–pH plots were examined visually, and various hydrolysis schemes were postulated to explain the data. Plausible sets of species and stability constants based on previous investigations (related by eq 1 and 2) were chosen as initial estimates for the least-squares regression of the $\bar{n}_o$ data. A value of $\bar{n}_o$ was calculated at each observation point according to the expression

$$\bar{n}_c = (\sum y Q_{x,y}[WO_4^{2-}]^x[H^+]^y)/m(WO_4^{2-}) \quad (7)$$

The free-tungstate concentration, $[WO_4^{2-}]$, was obtained by an iterative solution of the mass balance equation

$$[WO_4^{2-}] = m(WO_4^{2-}) - \sum x Q_{x,y}[WO_4^{2-}]^x[H^+]^y \quad (8)$$

and eq 7. The $Q_{x,y}$ values were then adjusted iteratively in eq 7 and 8 until a least-squares best fit to the observed data was obtained. The computer program used in this process was originally developed by Busing and Levy.[29] This program also calculates estimated errors and a correlation matrix for the $Q_{x,y}$ specified, as well as an agreement factor, $\sigma(\bar{n})$, defined by

$$\sigma(\bar{n}) = [(W(n_o - n_c)^2)/(N - N_v)]^{1/2} \quad (9)$$

where N, the number of observations, is usually much larger than N_v, the number of independent variables. The weight W is the squared reciprocal of the standard error of $\bar{n}_o$ calculated as the combined uncertainties in 17 independently measured quantities involved in the preparation of solutions and the measurement of potentials, temperatures, and volumes.

The goodness and uniqueness of fit of a proposed speciation scheme was judged according to the following criteria: (1) low $\sigma(\bar{n})$ values (If all errors in the 17 measured quantities were properly estimated and if the proposed scheme were correct, this value would approach unity. This quantity is minimized in the least-squares analysis.); (2) low standard errors in $Q_{x,y}$ and low correlation coefficients between these values; (3) randomness of the $\bar{n}_o - \bar{n}_c$ values as a function of pH.

The solid curves in Figures 1 and 2 represent a fit to the values calculated by regression according to hydrolysis scheme A, Table IV (see below). The $\bar{n}_o$–pH plots are generally quite smooth and behave systematically as a function of temperature and ionic strength. The fact that most of the curves represent data from two to four experiments attests to the reproducibility of the titrations.

Interpretation

General Observations. As discussed by Baes and Mesmer,[10] the shapes of $\bar{n}$–pH curves are indicative and, to a certain extent, diagnostic of the hydrolysis products formed during a titration. The shapes and spacings of the curves are a function of x, y, y/x (x and y defined as in eq 1), and the stoichiometric concentration of the metal or oxyanion undergoing hydrolysis. In particular, at a given temperature and ionic strength, monomeric species result in $\bar{n}$–pH curves that are coincident, regardless of the metal concentration. On the other hand, polynuclear hydrolysis products result in $\bar{n}$–pH curves that are concentration dependent.

The curves of Figure 1, where total tungsten concentration varied from 5×10^{-4} to 10^{-2} m, exhibit both types of behavior. The curves are not superimposed at all at 95 °C (Figure 1a). As temperature increases, a "mononuclear wall"[10] begins to develop in the low-$\bar{n}$ range. At 290 °C (Figure 1e) all of the curves are superimposed over a large $\bar{n}$ range. Thus, at least one other monomeric species besides WO_4^{2-} was formed in the runs, and at least one polynuclear species was also produced.

Another useful characteristic of $\bar{n}$ vs. pH curves is the occurrence of plateaus at $\bar{n}$ values of approximately y/x for each species formed, whenever the successive species' stability fields

(29) W. R. Busing and H. A. Levy, *Oak Ridge Natl. Lab.*, [*Rep.*] *ORNL-TM* (*U.S.*), ORNL-TM-271 (1963).

are sufficiently separated (1–2 pH units). Thus, each curve has a plateau at $\bar{n}_o = 0$, representing the field of stability of the $y/x = 0/1$ or WO_4^{2-} species, which is dominant in all solutions tested, above pH ~6. For the second monomer, there is obviously a plateau at $\bar{n}_o \approx 1.0$, best seen in the 290 °C runs (Figure 1e). This species is almost certainly the (1,1) or bitungstate ion, HWO_4^-.

Examination of the observed values of the curves of Figure 1 indicates plateaus or inflections at $\bar{n}_o \approx 1.2$ in the 95 °C runs, at $\bar{n}_o \approx 1.5$ in the 150 and 200 °C runs, where total tungstate concentration is 0.01 *m*, and at $\bar{n}_o \approx 1.6$–1.7 at 150 and 200 °C for total tungstate concentration 0.005 and 0.001 *m*. Several species besides (1,0) and (1,1) are necessary to explain these curves, and as discussed above, these species must be polynuclear. In addition, the $I = 5.12$ *m* runs (Figure 2b) require a species with $y/x \approx 2.0$.

Due to the strong dependence of the curves of Figure 1 on total tungsten concentration, polynuclear species with high x values are indicated. Our experiments did not cover a sufficient range in total tungsten concentration to unequivocally identify these species solely from a mathematical analysis of the data. Fortunately we can rely on previous studies to provide likely candidates for a hydrolysis scheme to explain the observed data.

Low-Temperature Studies. As discussed above, Sasaki's work[5,6] was interpreted in terms of a series of hexatungstates, notably including a (6,7) species ($y/x = 1.17$), a (6,9) species ($y/x = 1.5$), and a (6,10) species ($y/x = 1.67$). Aveston's more careful work,[8] including ultracentrifuge and Raman data, demonstrated a (12,14) species ($y/x = 1.17$) in addition to (6,7) in the lower n range and (12,18), a dodecatungstate ($y/x = 1.5$). Recent studies[30-32] have also suggested the existence of a (7,8) heptatungstate in solution ($y/x = 1.14$) and its corresponding sodium salt. Tytko and Glemser[11] also reviewed studies that propose a decatungstate, (10,16) ($y/x = 1.6$), which is found in some crystal structures and which appears to be more stable in solution at higher temperatures than at lower temperatures.

Thus, from previous studies, various hexanuclear ((6,y), where y = 6–10), a heptanuclear ((7,8)), a decanuclear ((10,16)), and two dodecanuclear ((12,14), (12,18)) species have been proposed by various researchers to explain the speciation of tungsten in aqueous solutions below 100 °C. None of these studies cover the temperature range of our experiments.

Species Selection. It is possible that the hydrolysis products generated in our experiments have no counterpart at low temperatures. However, to test all possible hydrolysis schemes involving at least two monomers and three polymers whose x values might range from 1 to 12 and y values from 0 to 24, including all combinations thereof, would not only be a tremendous task but would undoubtedly lead to many schemes that fit the data equally well and, considering the errors in our experimental data, possibly erroneous choices that fit the data better than the correct scheme. Thus, we chose to limit our considerations to those species reported in previous studies as discussed above and to vary the protonation of these species within reasonable limits, always keeping in mind the constraints imposed by the data.

Accordingly, the 13 sets of data at constant temperature and ionic strength were fitted with use of the least-squares technique described above, employing eq 7–9. A total of over 250 hydrolysis schemes were tested. The results of these fits, including the calculated $Q_{x,y}$, calculated errors, and agreement factors ($\sigma(\bar{n})$) are available as a supplement to this text (Table X, supplementary material).

Even with this restricted subset of possible species, it was neither relevant nor feasible to test all combinations at all temperatures and ionic strengths. Since the tungsten concentration was varied only in the 1.0 *m* NaCl solutions, schemes involving polynuclear species were extensively tested only for this medium Only those schemes compatible with the $I = 1.014$ *m* data were retained and tested on the data at other ionic strengths. In all cases, the smallest number of species necessary to explain all of the data at a particular temperature and ionic strength was favored. Adding an additional species would occasionally improve the fit marginally but would greatly increase the calculated standard error and covariance in the $Q_{x,y}$ values. This was interpreted as meaning either that the data were not sufficiently extensive or accurate to establish the existence of that species or that the species did not, in fact, contribute appreciably at the experimental conditions tested.

As discussed above, the $I = 1.014$ *m* data indicate the existence of at least two monomers, (1,0) and (1,1), as well as several polynuclear species. In Figure 1b,c, the observed $\bar{n}_o$ values of the runs at a total tungstate concentration of 0.01 *m* at 150 and 200 °C are seen to plateau at $\bar{n}_o \approx 1.5$. The plots of the observed values at lower concentrations cross the data points of the 0.01 *m* runs and flatten at $\bar{n}_o$ 1.6–1.7. These "crossovers" to a higher $\bar{n}$ value are indicative of formation of a species with a smaller number of tungsten atoms (and thus a smaller concentration dependence of the $\bar{n}$–pH curves) at the lower concentrations relative to the species responsible for the 0.01 *m* data, as discussed by Baes and Mesmer.[10] Since, in the $\bar{n}$–pH region of the crossover, monomer concentrations are shown to be insignificant in later analysis, this smaller species must be polynuclear. If the choices are limited to previously reported species, the (12,18) "metatungstate" with $y/x = 1.5$ seems the most likely species to explain the 0.01 *m* data, while a smaller species must be dominant at the lower tungsten concentrations.

The metatungstate anion ((12,18), $y/x = 1.5$), most likely formulated as $H_2W_{12}O_{40}^{6-}$, has the well-known "Keggin structure" in which the two protons occupy the central core of a cagelike framework of WO_6 octahedra.[9,11,33] This structure is also possessed by the numerous heteropolyanions of the form $X^{n+}W_{12-y}Mo_yO_{40}^{(8-n)-}$, where X = Si^{IV}, P^V, ..., etc., in which an XO_4 tetrahedron occupies the central position.[9,22] Gundlach and Thormann[34] report the persistence of silicotungstic acid, $H_4SiW_{12}O_{40}$, to temperatures in excess of 200 °C in acid solutions. Many of the Keggin-structure polytungstates, including the metatungstate ion, are readily reducible to intensely blue colored mixed-valence-state forms that can accept several electrons with no change in structure.[22,35] It is interesting to note that a reduction reaction of the form $H_2 + H_2W_{12}O_{40}^{6-} \rightleftarrows H_4W_{12}O_{40}^{6-}$, as discussed by Pope and Varga,[35] would be undetectable by our experimental technique.

Therefore the observed blue coloration of many of our quenched solutions, together with the peculiar stability of the Keggin-structure polyanions, and the plateaus at $\bar{n}_o = 1.5$ in our data with "crossovers" to a smaller polymer at lower concentrations strongly support the formation of the (12,18) metatungstate species in our experiments. More importantly, least-squares analysis of the $I = 1.104$ *m* data with the addition

(30) K. G. Burtseva, et al., *Russ. J. Inorg. Chem.* (*Engl. Transl.*), **26** (8), 1143 (1981).
(31) K. G. Burtseva, et al., *Sov. Phys.-Dokl.* (*Engl. Transl.*), **23** (11), 784 (1978).
(32) J. Fuchs and E.-P. Flindt, *Z. Naturforsch., B: Anorg. Chem., Org. Chem.*, **34B**, 412 (1979).
(33) J. F. Keggin, *Proc. R. Soc. London, Ser. A*, **144**, 75 (1934).
(34) H. Gundlach and W. Thormann, *Z. Dtsch. Geol. Ges.*, **112i**, 1 (1960).
(35) M. T. Pope and G. M. Varga, Inorg. *Chem.*, **5** (7), 1249 (1966).
(36) G. Goldstein, C. M. Wolf, and J. P. Schwing, *Bull. Soc. Chim. Fr.*, 1201 (1971).

Table V. Scheme B for WO_4^{2-} Hydrolysis in NaCl Solutions (Errors Represent 3σ)

		log $Q_{x,y}$[a]					agreement
I, m	T, °C	(1,1)	(1,2)	(7,8)	(7,12)	(12,18)	factor $\sigma(\bar{n})$
5.120	200.0	4.06 ± 0.12	7.64 ± 0.12			107.93 ± 1.50	1.997
	250.0	4.31 ± 0.09	7.42 ± 0.12				1.855
	290.0	4.46 ± 0.08	7.27 ± 0.11				1.094
1.014	95.0			55.81 ± 0.06		117.47 ± 0.27	2.513
	150.0	3.86 ± 0.12		51.49 ± 0.27	69.52 ± 0.33	111.39 ± 0.21	3.633
	200.0	4.17 ± 0.03		49.73 ± 0.24	66.84 ± 0.24	107.37 ± 0.15	2.745
	250.0	4.58 ± 0.03		50.16 ± 0.21	66.73 ± 0.24		2.585
	290.0	4.78 ± 0.03		51.24 ± 0.27	66.81 ± 0.36		2.949
0.104	150.0	4.09 ± 0.06				115.53 ± 0.18	0.435
	200.0	4.69 ± 0.03			71.09 ± 0.21		0.478
	250.0	5.22 ± 0.03			72.62 ± 0.39		0.638
	290.0	5.64 ± 0.03			74.87 ± 0.27		0.430

[a] Figures in parentheses are the x and y values, respectively, for each species.

Table VI. Scheme C for WO_4^{2-} Hydrolysis in NaCl Solutions (Errors Represent 3σ)

		log $Q_{x,y}$[a]					agreement
I, m	T, °C	(1,1)	(1,2)	(7,8)	(10,16)	(12,18)	factor $\sigma(\bar{n})$
5.120	200.0	4.06 ± 0.12	7.64 ± 0.12			107.93 ± 1.50	1.997
	250.0	4.31 ± 0.09	7.42 ± 0.12				1.855
	290.0	4.46 ± 0.08	7.27 ± 0.11				1.094
1.014	95.0			55.81 ± 0.06		117.47 ± 0.27	2.513
	150.0	3.85 ± 0.09		51.55 ± 0.15	96.67 ± 0.21	111.00 ± 0.42	2.321
	200.0	4.16 ± 0.03		49.84 ± 0.15	93.30 ± 0.21	106.36 ± 0.21	2.429
	250.0	4.57 ± 0.03		50.16 ± 0.27	92.24 ± 0.36		2.994
	290.0	4.78 ± 0.03		51.27 ± 0.27	93.03 ± 0.48		2.892
0.104	150.0	4.09 ± 0.06				115.53 ± 0.18	0.435
	200.0	4.68 ± 0.03			99.20 ± 0.18		0.314
	250.0	5.22 ± 0.03			101.85 ± 0.57		0.633
	290.0	5.64 ± 0.03			105.15 ± 0.45		0.488

of the (12,18) species significantly improves the fits up to 200 °C.

Small inflections in the $\bar{n}$ vs. pH curves also appear in the 95 °C runs (Figure 1a) at $\bar{n}_0 \approx 1.2$. Known species that could explain this effect are the widely accepted[5,8,11] paratungstate A anion, (6,7), usually formulated as $HW_6O_{21}^{5-}$, the heptatungstate, (7,8), analogous to the well-studied paramolybdate anion,[9,11] $Mo_7O_{24}^{6-}$, and the dodecatungstate, (12,14).[8] As pointed out by Tytko and Glemser,[11] extreme accuracy and extensive data are required to distinguish between these species, particularly the hexamer and heptamer, from potentiometric titrations alone. Indeed, the (6,7) and (7,8) species both fit the experimental data fairly well (Tables IV–VI). The (12,14) species does not produce good fits and was rejected as a possible species. Aveston's study[8] indicated that at 50 °C the (12,14) species was important only at high tungsten concentrations. Thus, it might be expected that at more elevated temperatures, with tungsten concentrations in the millimolal range, this species would become unstable relative to either the (6,7) or the (7,8) species.

The 0.005 and 0.001 m $\bar{n}_0$ curves at 150 and 200 °C (Figure 1b,c) rise steeply to a plateau at $\bar{n}_0 \approx 1.6$–1.7, crossing the 0.01 m data curves. Various hexa-, hepta-, deca-, and dodecanuclear species were tested, and as expected, no dodecanuclear species adequately fits these data. However, the (6,10), (7,12), and (10,16) species all gave reasonably good fits to the observed data (Tables IV–VI). Species (7,11), when substituted for species (7,12), also produced reasonable fits in many cases. However, this species produces a very poor fit when incorporated in the 200 °C, I = 1.014 m runs and was therefore rejected.

The data at I = 5.12 m (Figure 2b) indicate a species with $y/x \approx 2.0$. The logical choice for this species is (1,2), tungstic acid—H_2WO_4. Since the tungsten concentration was not varied at this ionic strength, fully protonated polynuclear species such as (6,12), (7,14), (12,24), ..., etc. could not be ruled out. However, such species have never been reported in the literature. Obviously, further experiments at different tungsten concentrations would be desirable to substantiate this assignment.

Thus, several compelling lines of evidence support the occurrence of the (1,0), (1,1), (1,2), and (12,18) species in several of the sets of isothermal, constant ionic strength experiments. Some combination of the species (6,7), (7,8), (6,10), (7,12), and (10,16) also seems likely in several of the data sets. Obviously all of these species are not required to explain the data at a particular temperature and ionic strength. In fact, most of the isothermal, constant ionic strength data sets can be adequately interpreted in terms of two to four species in addition to (1,0). It is not presently possible to judge the importance of all of the species listed above, including more or less protonated forms of the various polymers. However, without direct experimental evidence to the contrary, it seems reasonable to suggest that the simplest possible hydrolysis scheme, involving the smallest number of species that adequately explains all of the experimental data, is the logical choice.

In the selection of an overall speciation scheme, various chemical criteria were considered. Increasing temperature and decreasing tungsten concentration should favor monomers and small polynuclear species. It is unlikely that a particular species present at a given set of experimental conditions would fail to form at a somewhat higher temperature and then reappear at an even higher temperature. Also, the calculated $Q_{x,y}$ values should be smoothly varying functions of temperature and ionic strength, with the recognition that these are competing effects. Coulombic considerations alone suggest that increasing ionic strength should favor reactions with the highest net sum of the squares of the charges (products–reactants), ΔZ^2, while increasing temperature opposes this

effect through a decrease in the dielectric constant of water.

The (1,2) species, tungstic acid, was necessary to explain the data at $I = 5.12$ *m* (Figure 2b). This species was added to the schemes at $I = 1.014$ and 0.104 *m*, and fits with fairly low agreement factors were obtained at several temperatures at each ionic strength. For reactions involving monomers only, the value of $Q_{x,y}$ should decrease systematically with increasing ionic strength. As can be seen from Table IV, the $Q_{1,1}$ values are a smoothly varying function of temperature and have a predictable ionic strength dependence. However, the $Q_{1,2}$ values did not exhibit a reasonable trend with ionic strength. The changes in $Q_{1,2}$ with ionic strength were generally smaller than those of $Q_{1,1}$ (a fact not consistent with the larger ΔZ^2 value of −4 for formation of (1,2) compared with −2 for (1,1)) and were occasionally opposite in sign. When the (1,2) species was deleted from the hydrolysis schemes at $I = 1.104$ *m*, only slightly poorer fits to the data were obtained, and thus, the (1,2) species was rejected at this ionic strength. The species (6,10), (7,12), and (10,16) provided significantly better fits to the $I = 0.104$ *m* data than the (1,2) species, further supporting the exclusion of (1,2) from the hydrolysis schemes at low ionic strength. In this case, a critical analysis of the data enabled the selection between a monomeric and a polynuclear species, even though the metal concentration was not varied in the experiments.

The data at $I = 5.12$ *m*, $T = 150$ °C, and total tungstate concentration 10^{-3} *m* (Table III) were also analyzed with use of the procedure described above, and the species (1,0), (1,1), (1,2), (6,7), and (12,18) adequately explained the data. However, the calculated $Q_{x,y}$ for these species did not conform to the general tr of temperature and ionic strength dependencies of the same equilibria at other conditions. Also the results were incompatible with previous studies. Since strongly drifting emf's were encountered in this experiment and the data were not reproducible, we have excluded the results as these conditions from subsequent discussion. It seems likely that a previously unreported species with a high y/x ratio forms sluggishly at this temperature and ionic strength. Further experimentation is needed to establish the speciation at these conditions.

Summary of Selected Species. If we take into consideration these chemical criteria, the goodness of fit criteria outlined above, the results of previous studies, and the logical choice of the simplest scheme compatible with all available data, three possible speciation schemes emerge. Scheme A, summarized in Table IV, includes (1,0), (1,1), (1,2), (6,7), (6,10), and (12,18). The calculated curves of Figures 1 and 2 are derived from this set of species. This scheme provides a fairly good fit to the data, considering the uncertainties, over most of the range of experimental conditions. However, a plateau in the $I = 1.014$ *m* runs at 150 and 200 °C and total tungstate concentration 0.01 *m* is not predicted at $\bar{n}_c = 1.5$, as expected from the observed data. It is possible that the (12,18) species, once formed, remains metastably in solution, due to its inherently stable structure. Aveston's failure to detect a smaller polymer with $\bar{n} > 1.5$ in his 50 °C experiments may also have resulted from a similar kinetic barrier to the breakdown of the (12,18) species, once formed.

Schemes B and C provide very similar fits to the data, as shown in Tables V and VI. In scheme B, the species (6,7) and (6,10) are replaced by (7,8) and (7,12). In scheme C, (6,7) is replaced with (7,8) and (6,10) with (10,16). The combination of (6,7) with (10,16) provided a much poorer fit to the data and is not tabulated here.

Scheme A is slightly favored for several reasons, such as overall goodness of fit, support from previous studies, smaller overall standard errors in the estimated $Q_{x,y}$, and general simplicity. Although the (6,10) species is not well established in previous studies, fits that excluded this species in many cases produced very poor agreement factors or resulted in very large uncertainties in the formation constants of the remaining species. Thus, the data force us to include this species, despite the lack of experimental evidence for its existence, other than our own results.

Also, it it sensible to consider the W(VI) system in terms of six-tungsten species at low concentrations and high temperatures and twelve-tungsten species at high concentrations and low temperatures, along with the monomers. Reactions such as the slow conversion of (6,7) to (12,14) reported by Aveston[8] at 50 °C can then be considered as simple dimerization reactions, as discussed by Tytko and Glemser,[11] although M. T. Pope[37] has challenged the dimerization mechanism. However, there is no statistically justifiable basis for choosing scheme A over either scheme B or scheme C. All three hydrolysis schemes reflect consistent chemical behavior. The degree of polynucleation decreases with increasing temperature and decreasing tungsten concentration. Moreover, in each case, the $Q_{x,y}$ values vary systematically with temperature and ionic strength.

More detailed experimental studies might prove which, if any, of schemes A, B, and C is the correct hydrolysis scheme for W(VI) under these experimental conditions. However, an examination of Tables IV–VI reveals that the $Q_{x,y}$ values for (1,1) and (1,2) are virtually identical and the $Q_{12,18}$ values are very similar in all three schemes. The evidence for the existence of the (1,0) and (1,1) species is incontrovertible, and several lines of evidence support the (12,18) species. Since tungstic acid, (1,2), is the only known species that can explain the high-$\bar{n}$ data, the ambiguity involves only the assignment of the hexanuclear or heptanuclear species. Therefore, the stabilities of the tungsten monomers and the relative importance of polymers at high temperatures are well established.

Discussion

The species distribution diagrams in Figure 3 are drawn from the data of Table IV, hydrolysis scheme A. The figures are drawn at 150 and 290 °C, $I = 1.014$, and total tungstate concentrations of 10^{-2} and 10^{-3} *m*. Similar diagrams employing either scheme B (Table V) or scheme C (Table VI) differ essentially in the labels of the hexanuclear curves with (6,7) replaced by (7,8) and (6,10) by either (7,12) or (10,16). The shaded region in Figure 3a indicates the approximate pH range in which an unidentified solid is stable at these conditions. The strong concentration dependence of tungsten speciation is evident, particularly at 150 °C. Polynuclear species dominate the acid pH range at all temperatures when total tungstate concentration is 10^{-2} *m*, while the monomeric species become the major solution components over most of the pH range at a total tungstate concentration of 10^{-3} *m*. Comparison of parts a and c and parts b and d of Figure 3 shows that increasing temperature also has a strong effect on destabilization of polynuclear species. The ionic strength effects are much less dramatic.

Monomeric Species. 1. Tungstate–Bitungstate Equilibrium. As can be seen from Table IV, values of log $Q_{1,1}$ have been determined across most of the range of temperature and ionic strength in our experiments. In order to develop a functional relationship, eq 1 for species (1,1) was recast into the hydroxide form

$$H_2O + WO_4^{2-} \rightleftarrows HWO_4^- + OH^- \qquad (10)$$

$$Q'_{1,1} = Q_{1,1}Q_w = [HWO_4^-][OH^-]/[WO_4^{2-}] \qquad (11)$$

by adding the water dissociation reaction.

(37) M. T. Pope, private communication, 1983.

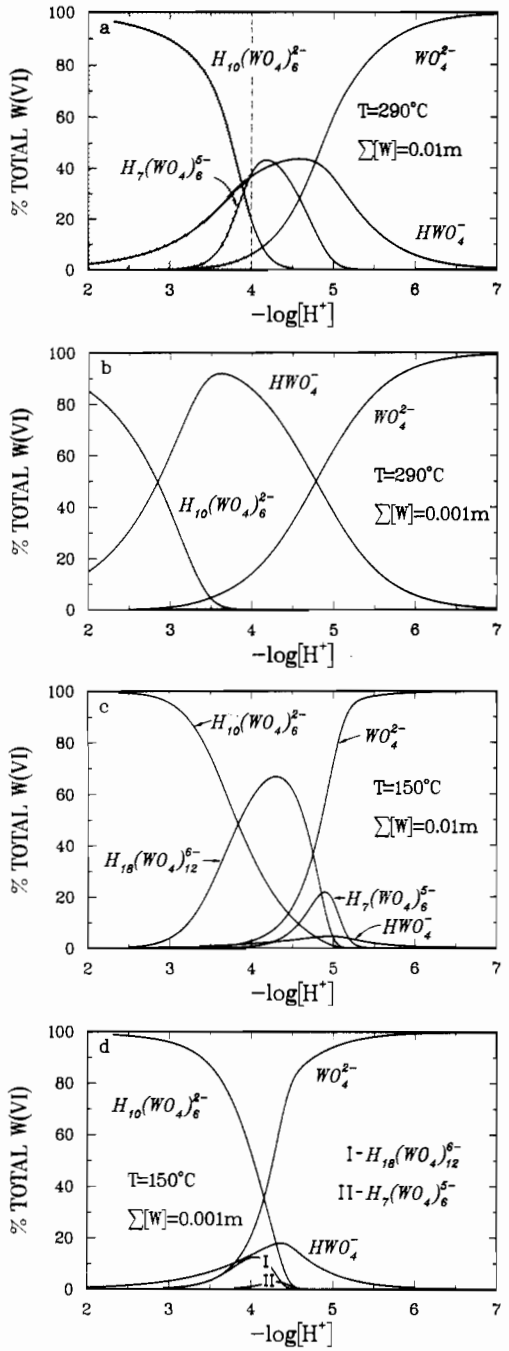

Figure 3. Speciation diagrams: (a) 0.01 *m* W(VI), 290 °C (shaded region represents metastable equilibria relative to unidentified solid); (b) 0.001 *m* W(VI), 290 °C; (c) 0.01 *m* W(VI), 150 °C; (d) 0.001 *m* W(VI), 150 °C. All plots are at I = 1.104 *m* and are generated from data in Table IV.

The reaction formulated according to eq 10 is expected to have a much smaller heat capacity and volume change than the same reaction formulated according to eq 1, as discussed by Lindsay[39] and others. Also, since ΔZ^2 for this reaction is −2, compared with −4 for the same reaction according to eq 1, the ionic strength dependence of $Q'_{1,1}$ should be simpler than that of $Q_{1,1}$.

Thus, values of log $Q'_{1,1}$ were obtained by adding to the log $Q_{1,1}$ data in Table IV the log Q_w results of Busey and Mesmer.[28] These values were then fitted to the equation (T, K; I, mol/kg)

$$\log Q'_{1,1} = p_1 + p_2/T + p_3 \ln T + \log a_{H_2O} - 2AI^{1/2}/(1 + I^{1/2}) + p_4 I + p_5 I T^2 + p_6 I[F(I)] \quad (12)$$

where $F(I)$ and the Debye–Hückel parameter A are defined as in previous studies[28] and log $a_{H_2O} = -0.0157\ \Phi I$ is calculated from the osmotic coefficient data for NaCl solutions reported by Liu and Lindsay.[44] The general form of eq 12 has been shown to adequately describe the temperature and ionic strength dependencies of numerous hydrolysis equilibria[25,28,40-42] and is discussed in detail by Busey and Mesmer.[40]

Least-squares regression of our data alone to eq 12 resulted in an agreement factor of 1.71 with deviations from the data of less than 2σ. Extrapolation to room temperature agreed fairly well with the data in Table I. In order to provide a more useful equation over the entire temperature range, some of the $Q_{1,1}$ values of Table I were incorporated in the regression analysis. The value of ~3.8 reported by Tytko and Glemser[16] in 3 *m* $NaNO_3$ does not agree with the other low-temperature results and neither the experimental technique nor the uncertainty of their results are reported. Thus only the values reported by Yatsimirskii and Romanov,[14] Schwarzenbach,[13] and Krumhansl[17] were used. The last value was determined from scheelite ($CaWO_4$) solubility studies at very low total tungsten concentrations. These three values for log $Q_{1,1}$ with arbitrary standard error assignments of σ = 0.20 log unit, together with the 11 values in Table IV, were fitted with use of eq 12 and an agreement factor of 1.63 was obtained. Regression of these 14 data points yields an equation that describes the entire data set to within 2σ and results in reduced uncertainties in $Q_{1,1}$ at low temperatures. The coefficients for eq 12 with these results are

$$p_1 = -28.577 \quad p_3 = 4.3418 \quad p_5 = 1.7499 \times 10^{-6}$$
$$p_2 = -1949.0 \quad p_4 = -0.35070 \quad p_6 = 1.4501$$

This equation was differentiated numerically in order to derive ΔH, ΔS, and ΔC_p for reaction 10. These derived properties were obtained with the assumption that ΔV for this reaction is zero. This assumption is justified as a first approximation in the absence of volume data, since the reaction is charge balanced with anions only, resulting in reduced volume changes associated with electrostriction.

Smoothed values for log $Q'_{1,1}$ and log $Q_{1,1}$, and ΔH, ΔS, and ΔC_p for the formation of (1,1) according to reaction 1 are given

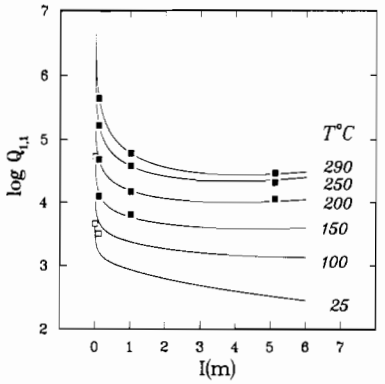

Figure 4. log $Q_{1,1}$–ionic strength plots at isotherms from 25 to 290 °C according to eq 1, 11, and 12: (■) data from the present study; (□) data from Table I (see text).

(38) R. Arnek, *Acta Chem. Scand.*, **23**, 1986 (1969).
(39) W. T. Lindsay, Jr., *Proc. Int. Water Conf., Eng. Soc. W. Pa.*, **41**, 284 (1980).
(40) R. H. Busey and R. E. Mesmer, *J. Solution Chem.*, **5** (2), 147 (1976).
(41) B. F. Hitch and R. E. Mesmer, *J. Solution Chem.*, **5** (6), 667 (1976).
(42) R. E. Mesmer and B. F. Hitch, *J. Solution Chem.*, **6** (4), 251 (1977).
(43) F. H. Sweeton, R. E. Mesmer, and C. F. Baes, Jr., *J. Solution Chem.*, **3** (3), 191 (1974).
(44) Chia-tsun Liu and W. F. Lindsay, Jr., *J. Solution Chem.*, **1**, 45 (1972).
(45) W. L. Marshall and C.-T. A. Chen, *Geochim. Cosmochim. Acta*, **46**, 289 (1982).

Table VII. Smoothed Thermodynamic Quantities for the Formation of Species (1,1), Bitungstate, according to Eq 1, Calculated from Eq 11 and 12[a]

T °C	$\log Q'_{1,1}$	$\log Q_{1,1}$	ΔH J/mole	ΔS J/(mole deg)	ΔC_p
		I=0.0m			
25	-10.38±.53	3.62±.53	6276±12872	90±33	314± 65
50	-9.52 .36	3.75 .36	13495 11286	114 28	269 65
100	-8.09 .16	4.17 .16	26291 8154	150 19	258 65
150	-6.92 .06	4.71 .06	40396 5153	186 11	316 65
200	-5.95 .04	5.34 .04	58684 2752	226 6	423 65
250	-5.12 .04	6.07 .04	83725 3088	276 6	593 65
300	-4.40 .06	6.89 .06	122107 5697	345 11	1045 65
		I=0.1m			
25	-10.56±.53	3.22±.53	4951±12877	78±33	294± 65
50	-9.71 .36	3.34 .36	11542 11293	100 28	239 65
100	-8.30 .16	3.70 .16	22453 8161	131 19	213 65
150	-7.18 .06	4.16 .06	33834 5151	160 11	248 65
200	-6.25 .03	4.68 .03	47281 2701	189 6	283 65
250	-5.50 .03	5.23 .03	60903 2972	217 6	243 64
300	-4.92 .05	5.76 .05	70607 5577	234 10	170 64
		I=0.5m			
25	-10.67±.53	3.03±.53	4566±12902	73±33	280± 64
50	-9.82 .37	3.14 .37	10709 11322	93 28	218 64
100	-8.41 .16	3.47 .16	20269 8196	121 19	180 64
150	-7.29 .06	3.88 .06	29692 5174	144 11	199 64
200	-6.37 .03	4.33 .03	39628 2614	167 5	181 64
250	-5.65 .03	4.77 .03	44877 2684	177 5	-15 64
300	-5.13 .04	5.09 .04	33108 5267	155 10	-497 64
		I=1.0m			
25	-10.78±.54	2.94±.54	4908±12936	73±33	273± 64
50	-9.93 .37	3.04 .38	10837 11365	92 28	207 64
100	-8.50 .17	3.37 .17	19747 8261	117 19	165 64
150	-7.36 .07	3.76 .07	28223 5275	139 11	176 63
200	-6.42 .04	4.18 .04	36439 2779	157 6	131 63
250	-5.68 .03	4.57 .03	37516 2803	159 5	-144 63
300	-5.17 .04	4.80 .04	14762 5309	118 10	-845 63
		I=3.0m			
25	-11.28±.68	2.69±.60	7588±13110	77±33	263± 63
50	-10.37 .44	2.83 .44	13209 11605	95 28	193 63
100	-8.84 .24	3.20 .24	21171 8745	118 20	142 64
150	-7.58 .13	3.61 .13	28247 6354	136 13	140 65
200	-6.52 .08	4.01 .08	33841 5255	148 10	53 66
250	-5.65 .04	4.35 .04	28331 6347	137 12	-352 69
300	-5.03 .07	4.45 .07	-12613 9031	63 17	-1442 73
		I=5.0m			
25	-11.77±.70	2.52±.70	10750±13343	84±33	260± 64
50	-10.81 .54	2.70 .54	16265 11953	102 28	187 64
100	-9.17 .35	3.14 .35	23887 9538	124 20	134 67
150	-7.77 .23	3.59 .23	30444 8142	141 16	127 71
200	-6.57 .14	4.02 .14	34995 8581	151 16	21 77
250	-5.54 .08	4.36 .08	26666 10974	134 21	-443 84
300	-4.75 .13	4.43 .13	-22702 14746	45 28	-1731 94

[a] Equilibrium quotients are tabulated for the formation of bitungstate according to reaction 10 ($\log Q'_{1,1}$) and reaction 1 ($\log Q_{1,1}$).

in Table VII at 50 °C intervals from 0 to 300 °C at six ionic strengths. All listed uncertainties represent three times the computed standard error. Thermodynamic data for the reaction written according to eq 10 are tabulated in the supplementary material of this paper (Table IX) and can be obtained by simply adding to the data in Table VII the corresponding values for water dissociation tabulated by Busey and Mesmer.[28] The $\log Q_{1,1}$ and $\log Q'_{1,1}$ values from eq 12 are compared with the experimental points in Figures 4 and 5. As can be seen, the temperature and ionic strength dependences of $\log Q'_{1,1}$ are much simpler than those of $\log Q_{1,1}$ and our choice of fitting the hydroxide form (eq 10) appears justified.

The large uncertainties in the thermodynamic data in Tables VII and IX are mainly due to the small number of observations (14) relative to the number of adjustable parameters in eq 12 and the large standard errors assigned to the $Q_{1,1}$ values at low temperature. Since no experimentally derived thermodynamic quantities for this equilibrium have been previously reported, they are tabulated here despite the large uncertainties.

In order to formulate eq 4, Ivanova and Khodakovskiy[3,18] assumed for the reaction $HWO_4^- \rightleftarrows H^+ + WO_4^{2-}$ the following thermodynamic values, based on a comparison with numerous other inorganic acids: $\Delta H°_{298.15} = -16.217$ kJ/mol, $\Delta S°_{298.15} = -126 \pm 13$ J/(mol deg), and $\Delta C_p°_{298.15} = -228$ J/(mol deg). Using eq 11 and 12, we compute the following values for the same reaction at $I = 0.0$ and $T = 298.15$ °C: $\Delta H = -6 \pm 13$ kJ/mol, $\Delta S = -90 \pm 33$ J/(mol deg), and $\Delta C_p = -314 \pm 65$ J/(mol deg). Values of $\log K_{1,1}$ from this study (Table VII, $I = 0.0$) and those of Ivanova and Khodakovskiy[3] (eq 4) are plotted as a function of temperature in Figure 6. The curves are essentially the same at $T < 100$ °C, within the uncertainty of our extrapolation, but there is a systematic deviation increasing to about 1 log unit from 200 to 300 °C. Considering that eq 4 was derived from extrathermodynamic empirical relationships, this deviation is not surprising.

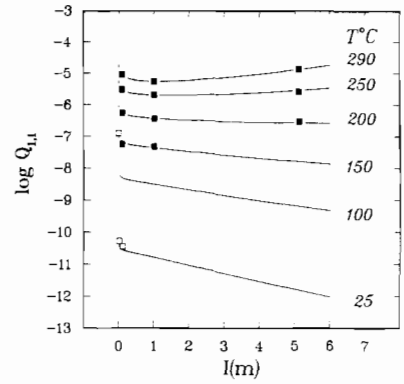

Figure 5. $\log Q'_{1,1}$–ionic strength plots at isotherms from 25 to 290 °C according to eq 12: (■) data from the present study; (□) data from Table I (see text).

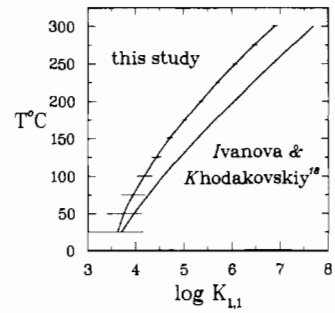

Figure 6. $\log K_{1,1}$ from this study (Table VII, $I = 0$) and from Ivanova and Khodakovsky (eq 4) vs. temperature. The horizontal error bars on $\log K_{1,1}$ represent 3σ.

2. Sodium Ion–Tungstate Interaction. If eq 10 is written in reverse order, $\Delta Z^2 = 2$ and the activity coefficient ratio can be expressed as

$$(\gamma_{WO_4^{2-}}/\gamma_{OH^-}\gamma_{HWO_4^-}) = Q'_{1,1}/(K'_{1,1}a_{H_2O})$$

Other reactions for which $\Delta Z^2 = 2$ and for which extensive data are available over a broad range of temperatures and ionic strengths include the dissociation of water in NaCl media[28] and the second dissociation of phosphoric acid in KCl solutions[26] written in the hydroxide form. In these cases, $\gamma_{H^+}\gamma_{OH^-} = K_w a_{H_2O}/Q_w$ and $\gamma_{HPO_4^{2-}}/(\gamma_{OH^-}\gamma_{H_2PO_4^-}) = Q_2/(K_2 a_{H_2O})$. With use of the approximation suggested by Lindsay[39] that

$$\gamma_{X^z} = \gamma_{\pm NaCl}{}^{z^2}$$

where z is the charge on the ion, all of these activity coefficient ratios can be approximated by $\gamma_{\pm NaCl}{}^2$. These activity coefficient quotients are compared with $\gamma_{\pm NaCl}{}^2$ in Table VIII. Errors in the tungstate ratio are approximately 0.1 unit over most of the range. The errors in the other tabulated quantities are considerably less than this.

There is no significant difference between these values at $I = 0.1$ *m*. At $I = 1.0$ *m*, the phosphate ratio remains fairly close to $\gamma_{\pm NaCl}{}^2$ and $\gamma_{H^+}\gamma_{OH^-}$. Mesmer and Baes[26] used this argument, together with the very small ionic strength dependence of the first dissociation of phosphoric acid written in

Table VIII. Activity Coefficient Ratios[a] for Reactions with $\Delta Z^2 = 2$: $A = \gamma_{\pm NaCl^2}$, $B = \gamma_{WO_4^{2-}}/(\gamma_{OH^-}\gamma_{HWO_4^-})$, $C = (\gamma_{H^+}\gamma_{OH^-})_{NaCl}$, $D = (\gamma_{HPO_4^{2-}}/\gamma_{OH^-}\gamma_{H_2PO_4^-})_{KCl}$

T, °C	A	B	C	D
		$I = 0.1$ *m*		
100	0.56	0.61	0.55	0.52
150	0.50	0.56	0.49	0.49
200	0.44	0.50	0.43	0.45
250	0.36	0.42	0.34	0.40
300	0.26	0.31	0.24	0.33
		$I = 1.0$ *m*		
100	0.39	0.40	0.39	0.24
150	0.31	0.38	0.29	0.21
200	0.22	0.35	0.20	0.18
250	0.14	0.28	0.11	0.15
300	0.07	0.17	0.05	0.13
		$I = 5.0$ *m*		
100	0.64	0.10	0.89	
150	0.40	0.17	0.43	
200	0.22	0.29	0.16	
250	0.10	0.45	0.04	
300	0.03	0.51	0.01	

[a] Sources of information: *A*, ref 44; *B*, this study (Table VII); *C*, ref 28; *D*, ref 26.

the hydroxide form, to suggest that pairing of K^+ with HPO_4^{2-} is minor and insignificant with $H_2PO_4^-$ over their experimental range. The value $\gamma_{\pm NaCl}^2 - (\gamma_{WO_4^{2-}}/\gamma_{OH^-}\gamma_{HWO_4^-})$ decreases sharply with increasing ionic strength above 200 °C, suggesting that the interaction of Na^+ with WO_4^{2-} is weaker on an isocoulombic basis than with OH^- or Cl^-. This comparison may be a reflection of inherent difficulties in relating the $\gamma_\pm$ of a 1:1 electrolyte to activity coefficient quotients of equilibria with a doubly charged ion. At any rate the interaction of ions in the $Q_{1,1}$ equilibrium with Na^+ are weak relative to the Na–Cl interaction at high temperatures and ionic strengths.

Polynuclear Species. The log $Q_{x,y}$ data for the polynuclear species in 1 *m* NaCl listed in Table IV are plotted as a function of temperature in Figure 7. Also plotted are all previously reported values for the association constants of these species in various ionic media. Our results at other ionic strengths are not plotted since the data are not as extensive and have not been verified by varying the tungsten concentration. There are no reported values with which to compare the $Q_{x,y}$ values for species (7,8), (7,12), or (10,16) listed in Tables V and VI.

The data in Table IV for the 1 *m* NaCl solutions were fitted to equations of the form (T, K)

$$\log Q_{x,y} = A + B/T + C \ln T - y \log Q_w \qquad (13)$$

for the species (6,10) and (12,18) in 1 *m* NaCl. The last term was introduced in order to transform the $Q_{x,y}$ data into constants for the hydroxide form for interpolation. The log $Q_{12,18}$ value of 132.51 reported by Aveston[8] in 3 *m* LiCl at 50 °C was included in the fit to the (12,18) data. To account for the uncertainty introduced by fitting the data of different ionic media to a media-independent equation, a large and arbitrary standard error of 0.3 log unit was assigned to Aveston's $Q_{12,18}$ value. These equations are plotted as the solid curves in Figure 7. These curves fit the results of our study for the species (6,10) well within the uncertainty listed in Table IV. The fit to the (12,18) data is considerably poorer, as can be seen from Figure 7. This may be due to the large influence of Aveston's[8] result in a totally different ionic medium.

According to these extrapolations, Aveston[8] should have detected the species (6,10) at 50 °C, if the ionic strength dependence of this species is small. However, examination of Table IV indicates that, upon an increase of the ionic strength from 0.104 to 1.014 *m*, the formation constants for the species (6,10) *decrease* by about 7 log units at 290 °C and

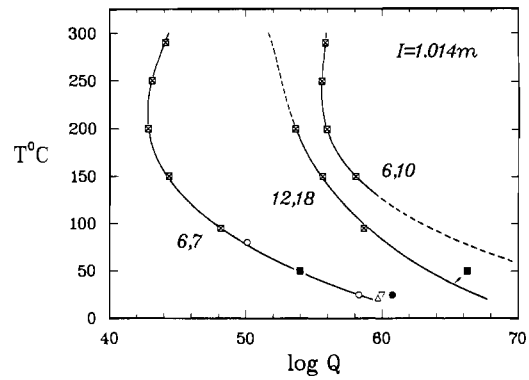

Figure 7. Equilibrium quotients (log Q) for the (6,7), (6,10), and (12,18) species (log $Q_{12,18}$ values multiplied by 0.5). Symbols for the data are as follows: (⊠) Table IV, this study; (○) Sasaki,[6] 1.0 *m* $NaClO_4$; (■) Aveston,[8] 3 *m* LiCl; (△) Tytko and Glemser,[16] 3 *m* $NaNO_3$; (▽) Goldstein et al.,[36] 3 *m* NaCl; (●) Arnek and Sasaki,[7] 3 *m* $NaClO_4$. Smoothed curves are from eq 13 for (6,10) and (12,18) and eq 14 for (6,7).

4 log units at 150 °C. There appears to be a (somewhat smaller) decrease in the constants for (12,18) as well, although the data are insufficient for predictive purposes. Thus, it appears that ionic strength effects are large for these species. Because very few data are available on the behavior of large, highly charged polynuclear species in ionic media at elevated temperatures, it is impossible to compare the different media effects of 1 *m* NaCl and 3 *m* LiCl on the formation constants of these polynuclear species when there are no data for both media at any one temperature.

Since our data for $Q_{6,7}$ agreed quite well with those of previous studies, we included Sasaki's[6] results for log $Q_{6,7}$ in 1 *m* $NaClO_4$ at 25 and 80 °C (58.3 and 50.1, respectively), with an arbitrary standard error assignment of ±0.10 log unit, together with our results in 1 *m* NaCl and fitted the data to an equation of the form (T, K)

$$\log Q_{6,7} = A + B/T + C \ln T + DT - 7 \log Q_w \qquad (14)$$

which is also plotted in Figure 7. This equation fits our experimental points for the species (6,7) well within the uncertainty listed in Table IV. The constants in eq 13 and 14 are

	log $Q_{6,7}$ (eq 14)	log $Q_{6,10}$ (eq 13)	log $Q_{12,18}$ (eq 13)
A	876.08	−525.43	132.16
B	−26 717	19 502	−32 617
C	−158.526	70.471	−23.845
D	0.265 05		

Thermodynamic data for (6,7) polynucleation were obtained by numerical differentiation of eq 14 assuming that the ΔV for the reaction is equal to $-7(\Delta V_w)$ (approximate values of ΔV are needed for evaluation of constant-pressure derivatives). At $T = 298.15$ K and $I = 1.014$ *m*, we calculate, for species (6,7), $\Delta H = -389 \pm 56$ kJ/mol and $\Delta S = -183 \pm 162$ J/(mol deg). Arnek[38] reports values of $\Delta H°_{298.15} = -2.62 \pm 4$ kJ/mol and $\Delta S° = 285 \pm 13$ J/(mol deg) for the (6,7) reaction in 3 *m* $NaClO_4$ from calorimetric titrations. These results do not agree even within the large uncertainties in our extrapolated quantities. However, Arnek[38] assumed that formation of species (6,6) accompanied formation of (6,7) at 25 °C and 3 *m* $NaClO_4$, because this gave a better least-squares fit to Arnek and Sasaki's[7] potentimetric data in the same medium. Our data do not indicate the formation of both (6,6) and (6,7), at least at temperatures greater than 95 °C.

Conclusions

(1) The important tungsten(VI) species in sodium chloride solutions in the range $T = 95$–290 °C, $I = 0.1$–5.1 *m*, and total

tungsten concentration 10^{-2}–5×10^{-4} *m* are WO_4^{2-}, HWO_4^-, and H_2WO_4 and the polynuclear species (6,7), (6,10), and (12,18). The 12-tungsten species is not stable above 200 °C while the 6-tungsten species persist to 290 °C in the more concentrated solutions. The equilibrium quotients relating these species have been determined as a function of temperature and ionic strength, as summarized in Table IV.

(2) Reduction of tungsten(VI) to lower valence states was observed but was determined to be stoichiometrically insignificant at the experimental conditions and H_2 pressures of 0.7–3.5 MPa.

(3) Ion pairing of Na^+ with HWO_4^- and WO_4^{2-} is apparently less extensive than with either OH^- or Cl^- on an isocoulombic basis.

(4) Hydrous sodium polytungstates precipitated during some of the runs at high total tungsten concentrations. These solids exhibit retrograde solubilities. One solid, identified by X-ray diffraction analysis, was $Na_2O{\cdot}(WO_3{\cdot}{}^1/_2H_2O)_{8\text{–}40}$, tungsten phase C of Freedman and Leber.[20]

(5) From Figure 3 and Table IV, it is apparent that in near-neutral, mildly to strongly saline, 150–300 °C solutions at total tungsten concentrations of 10^{-4}–10^{-5} *m*, the most important tungsten species will be tungstate (WO_4^{2-}) and bitungstate (HWO_4^-). Tungstic acid will be important only at low pH values. Consequently the most significant equilibrium to be considered in tungsten ore-depositing solutions is $H^+ + WO_4^{2-} \rightleftarrows HWO_4^-$. Equations 11 and 12 provide the means of calculating this equilibrium in the range 25–300 °C, I = 0–5.12 *m*.

Acknowledgment. This research was supported by Oak Ridge Associated Universities, the Division of Engineering, Mathematical, and Geosciences, Office of Basic Energy Sciences, U.S. Department of Energy, under Contract W-7405-eng-26 with the Union Carbide Corp. and by National Science Foundation Grant EAR-80-07839 (H.O.).

Registry No. W, 7440-33-7; WO_4^{2-}, 14311-52-5.

Supplementary Material Available: Tables IX (smoothed thermodynamic parameters for the formation of species (1,1), bitungstate, according to eq 1) and X (hydrolysis schemes tested on the data of Tables II and III by using eq 8–10) (11 pages). Ordering information is given on any current masthead page.

Contribution from the Department of Chemistry, Georgetown University, Washington, D.C. 20057

Kinetics of the Reaction of the Bis(μ-oxalato)bis(μ-acetato)diaquodiruthenium(II,III) Anion with $Ti(H_2O)_6^{3+}$

RATHINDRA N. BOSE, PAUL A. WAGNER, and JOSEPH E. EARLEY*

Received July 15, 1983

Reduction of $Ru_2(CH_3COO)_2(C_2O_4)_2(H_2O)_2^-$ by Ti^{3+} (at 25 °C, in 1.0 M $LiCF_3SO_3$) involves formation of an intermediate containing two ruthenium atoms and one titanium atom (K_f = ca. 3×10^2 M^{-1}). Intramolecular electron transfer within the conjugate base of that intermediate has a rate constant of 3×10 s^{-1}. The relatively slow rate of intramolecular ET is ascribed to energy mismatch between electron-donor and -acceptor orbitals.

In previous papers,[1] we have established that electron-transfer (hereafter, ET) reactions having Ru(III) complexes as oxidants and Ti(III) species as reductants involve a variety of mechanisms. In the absence of suitable bridging groups, outer-sphere ET occurs if an electron-delocalizing ligand is present on either redox partner. If a ligand with an open coordination position, and a π-electron system that facilitates overlap between electron-donor and electron-acceptor orbitals, is present on the oxidant, then an inner-sphere mechanism prevails and the rate-limiting step is formation of the binuclear activated complex. There is evidence for rate-limiting ET if 3-formylpentane-2,4-dione is the bridging ligand. Carboxylate ligands are efficient bridges and give rise to substitution-limited reactions. Wieghardt, Sykes, and their co-workers[2] have used binuclear μ-carboxylato Co(III) complexes to study the ET through intervening groups, in reactions in which the reductant attacks at a lead-in group remote from the site of coordination of the bridging group to the oxidant metal atom. For μ-carboxylato complexes, attack of the reductant at the uncoordinated oxygen atom of the coordinated carboxyl group is forestalled by the second metal atom.

Recently, μ-carboxylato complexes containing two ruthenium atoms have been the subject of intense study. Particular attention has been given to metal–metal bonding in such complexes.[3] Diruthenium complexes studied heretofore have not contained noninsulating ligands that also included remote lead-in groups. We set out to synthesize complexes that would make it possible to study Ru(III)–Ti(III) ET reactions that are mediated by carboxylate ligands in which adjacent attack on oxygen was blocked by coordination. Our previous work has shown that oxalate was an effective mediator of Ru(III)–Ti(III) ET both when monocoordinated and when bicoordinated. This paper provides evidence that ET from Ti(III) through the remote carboxyl group of a μ-oxalato ligand bridging two ruthenium atoms is slower than the corresponding reaction of monomeric oxidants.

Experimental Section

Initial attempts to substitute oxalate for acetate in $Ru_2(CH_3COO)_4Cl$ yielded a variety of products; some of these were monomeric and others were dimers with one oxalate per dimer unit.[1b]

Bis(μ-oxalato)bis(μ-acetato)diaquodiruthenium(II,III) Acid Dihydrate. $Ru_2(CH_3COO)_4Cl$ (0.2 g) was added to a solution made by dissolving 0.15 g of oxalic acid in 200 mL of water. The solution was allowed to stand at room temperature until no further change

(1) Earley, J. E.; Bose, R. N.; Berrie, B. B. *Inorg. Chem.* **1983**, *22*, 1836. (b) Earley, J. E.; Berrie, B.; Barone, P.; Bose R. N.; Lee, R. A. *Coord. Chem.* **1980**, *21*. (c) Lee, R. A.; Earley, J. E. *Inorg. Chem.* **1981**, *20*, 1739. (d) Barone, P. A.; Earley, J. E., in preparation. (e) Hari Prasad, V. N.; Earley, J. E., work in progress. (f) Bose, R. N.; Earley, J. E. *J. Chem. Soc., Chem. Commun.* **1983**, 59. (g) Ali, S. Z.; Chalilpoyil, P.; Earley, J. E. *Inorg. Chim. Acta* **1981**, *48*, 57. (h) Berrie, B. B.; Earley, J. E. *Inorg. Chem.* **1984**, *23*, 774.

(2) E.g.: Hery, M.; Wieghardt, K. *Inorg. Chem.* **1978**, *17*, 1130.

(3) E.g.: Cotton, F. A. *J. Mol. Struct.* **1980**, *59*, 97.

0020-1669/84/1323-1132$01.50/0 © 1984 American Chemical Society